Aus dem Pathologischen Institut der

Ludwig-Maximilians-Universität München

Direktor: Prof. Dr. med. Thomas Kirchner

Arbeitsgruppe Experimentelle und Molekulare Pathologie

Leiter: Prof. Dr. rer. nat. Heiko Hermeking

Regulation of EMT and metastasis by mutual inhibition of AP4 and miR-15a/16-1 in colorectal cancer

Dissertation zum Erwerb des

Doktorgrades der Naturwissenschaften (Dr. rer. nat.)

an der Medizinischen Fakultät

der Ludwig-Maximilians-Universität München

vorgelegt von

Lei Shi

aus Hebei, Volksrepublik China

2014

Gedruckt mit der Genehmigung der Medizinischen Fakultät

der Ludwig-Maximilians-Universität München

Betreuer: Prof. Dr. rer. nat. Heiko Hermeking

Zweitgutachter: Prof. Peter Nelson

Dekan: Prof. Dr. med. Dr. h. c. Maximilian Reiser, FACR, FRCR

Tag der mündlichen Prüfung: 10.11.2014

Eidesstattliche Versicherung

Ich erkläre hiermit an Eides statt, dass ich die vorliegende Dissertation mit dem Thema

„ Regulation of EMT and metastasis by mutual inhibition of AP4 and miR-15a/16-1 in colorectal cancer ”

selbständig verfasst, mich außer der angegebenen keiner weiteren Hilfsmittel bedient und alle Erkenntnisse, die aus dem Schrifttum ganz oder annähernd übernommen sind, als solche kenntlich gemacht und nach ihrer Herkunft unter Bezeichnung der Fundstelle einzeln nachgewiesen habe.

Ich erkläre des Weiteren, dass die hier vorgelegte Dissertation nicht in gleicher oder in ähnlicher Form bei einer anderen Stelle zur Erlangung eines akademischen Grades eingereicht wurde.

München, den 3.7.2014

Lei Shi

To my parents, for their unconditional love, endless support and encouragement!

Table of Contents

Abbreviations **1**

1 Introduction **3**

1.1 The biology of cancer 3

1.2 EMT and cancer 4

1.3 The biology of colorectal cancer 6

1.4 p53 7

1.4.1 p53 enters the microRNA world 7

1.5 microRNAs and cancer 7

1.5.1 The biogenesis of miRNAs 8

1.5.2 miRNAs and diseases 9

1.5.3 miRNAs and cancer 10

1.6 The miR-15a/16-1 family 13

1.7 The transcription factor AP4 14

1.8 The transcription factor MYC 15

1.9 Aims of the Study 16

2 Materials **17**

2.1 Human cancer cell lines 17

2.2 Chemicals 17

2.2.1 General chemicals 17

2.2.2 Cell culture materials 18

2.2.3 Cell culture medium 19

2.2.4 Cell storage medium 19

2.2.5 Vectors 20

2.2.6 Materials for transfection and real time PCR 20

2.2.7 Materials for Western blot, flow cytometry and immunofluorescence 21

2.2.8 Materials for migration, invasion and would healing 25

2.2.9 Materials for cloning and dual-reporter luciferase assays 26

2.2.10 Oligonucleotides used for cloning and site-directed mutagenesis 27

2.2.11 Oligonucleotides used for qPCR analyses 28

2.2.12 Oligonucleotides used for qChIP analyses 28

2.2.13 Antibodies used for Western blot (WB) and immunofluorescence (IF) analysis 29

2.3 Materials for animal experiments 29

2.4 Colon cancer samples 30

2.5 Equipment 30

3 Methods 32

3.1 Cell culture 32

3.1.1 Starting cell culture from frozen cells 32
3.1.2 Subculture of adherent cell lines 32
3.1.3 Cell counting 32
3.1.4 Cell storage 33
3.1.5 Transfection of oligonucleotides, vectors and constructs 33
3.1.6 Generation of cell pools with conditional vectors 34

3.2 Generation of the *AP4* 3'-UTR constructs 34

3.2.1 Clone the *AP4* 3'-UTR constructs 34
3.2.2 Colony PCR 35
3.2.3 Ligation method 35
3.2.4 Transformation of heat shock-competent *E. Coli* XL1 blue 35
3.2.5 Purification of plasmid DNA from *E.coli* 36
3.2.6 Sequencing 37
3.2.7 Enzyme Restriction 37

3.3 Dual-reporter luciferase assays 37

3.4 RNA isolation and Quantitative real-time PCR 38

3.4.1 Isolation of RNA and reverse transcription reaction 38
3.4.2 Quantitative real-time PCR (qPCR) 39

3.5 Protein extraction and Western blot analysis 39

3.5.1 Protein extraction 39
3.5.2 Western blot analysis 40

3.6 Boyden-chamber assay of migration and invasion 41

3.7 Immunofluorescence and confocal laser-scanning microscopy 42

3.8 DNA content analysis by flow cytometry 42

3.9 Analysis of colon cancer samples 43

3.10 Statistical analyses 43

4 Results 44

4.1 p53 mediates down-regulation of AP4 after DNA damage 44

4.2 AP4 is a direct target of miR-15a and miR-16-1 45

4.3 p53 decreases AP4 by p53 via miR-15a/16-1 50

4.4 miR-15a/16-1 induces MET by repressing AP4 52

4.5 Role of AP4 in cell cycle inhibition by *miR-15a/16-1* 58

4.6 miR-15a/16-1 represses metastasis of CRC Xenografts 59
4.7 AP4 directly represses miR-15a/16-1 63
4.8 Inverse correlation between AP4 and miR-15a/16-1 expression in primary CRC 65
5 Discussion 68
5.1 p53-regulated miRNAs target transcription factors to regulate EMT 68
5.2 Repression of miR-15/16-1 by AP4 70
5.3 The role of the miR-15a/16-1/AP4 axis in EMT 71
5.4 The role of miR-15a/16-1/AP4 axis in cell cycle regulation 72
5.5 The role of miR-15a/16-1/AP4 axis in experimental tumors 73
5.6 The correlation of miR-15a/16-1 and AP4 in clinical samples 74
5.7 miR-15a/16-1, AP4 and future perspective 75
6 Summary 76
7 Zusammenfassung 77
8 Publications 79
9 References 80
Acknowledgment 91
Curriculum Vitae 92

Abbreviations

Abbreviation	Full name
3’-UTR	3’-untranslated region
APS	ammonium peroxodisulfate
bHLH	basic helix-loop-helix
CSC	cancer stem cell
CDH1	cadherin 1
cDNA	complementary deoxyribonucleic acid
ChIP	chromatin immunoprecipitation
CLL	chronic lymphocytic leukemia
CRC	colorectal cancer
DAPI	4',6-diamidino-2-phenylindole
DLEU2	deleted in lymphocytic leukemia 2
DMEM	Dulbecco's Modified Eagle Medium
DMSO	dimethyl sulfoxide
dNTPs	deoxynucleotide triphosphates
DOX	doxycycline
DOXO	doxorubicin
EMT	epithelial-mesenchymal transition
FBS	fetal bovine serum
GFP/RFP	green/red fluorescent protein
H&E	hematoxylin and eosin
IF	immunofluorescence
MDM2	mouse double minute 2 homolog
MET	mesenchymal-epithelial transition
miRNA	microRNA

MYC	myelocytomatosis oncogene
NOD/SCID	non-obese diabetic/severe combined Immunodeficient
PCR	polymerase chain reaction
PI	propidium iodide
pre-miRNA	precursor microRNA
pri-miRNA	primary microRNA
qPCR	quantitative polymerase chain reaction
RIPA	radio immunoprecipitation assay
RISC	RNA-induced silencing complex
SD	standard deviation
SDS	sodium dodecyl sulfate
TEMED	tetramethylethylenediamine
TFAP4	transcriptional factor activating enhancer binding protein 4
TGF-β	transforming growth factor-β
VIM	Vimentin
ZEB1	zinc finger E-box binding homeobox 1

1 Introduction

1.1 The biology of cancer

Only a small number of the approximately 25,000 genes in the human genome has been linked to cancer. Alterations in the same gene are often associated with different forms of cancer. These genes can be divided into three main functional groups.

The first group, called proto-oncogenes, produces protein products that normally enhance cell division or inhibit normal cell death. Proto-oncogene proteins inhibit apoptosis and senescence of cancer cells. They also promote cancer progression by promoting migration/invasion, angiogenesis and metastasis. The mutated forms of these genes are called oncogenes (Figure 1A) (Akinyeke et al., 2013; Cader et al., 2013). The second group, known as tumor suppressors, encodes proteins that normally prevent cancer cells division or cause cell death (Figure 1A) (Cader et al., 2013; Chen et al., 2013b). In tumor cells tumor suppressor genes loose their functions by mutation or inactivation by viral or epigenetic mechanisms. The third group of cancer causing genes is represented by DNA repair genes, which help prevent mutations that result in cancer (Park et al., 2013).

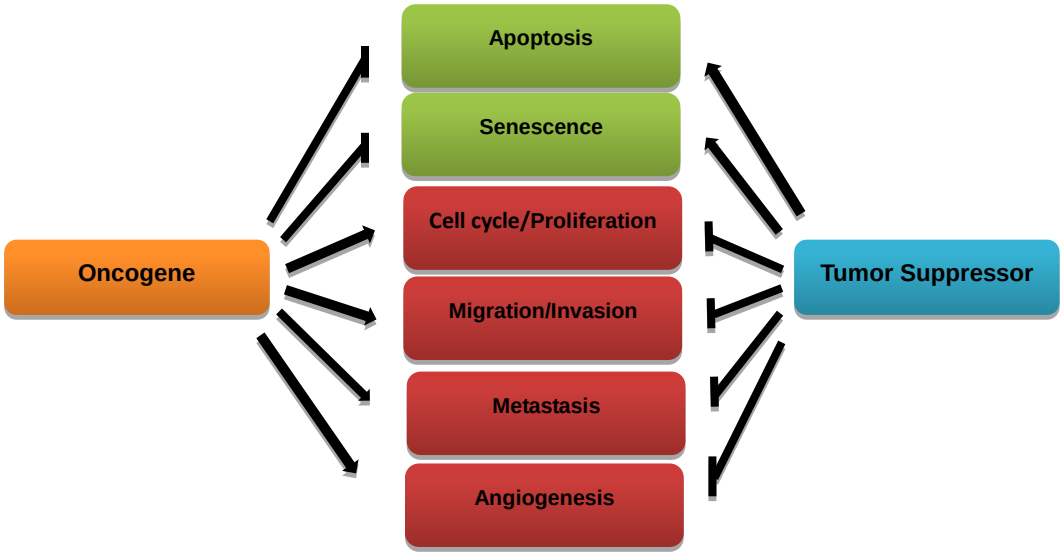

Figure 1 Oncogenes and tumor suppressors

The main functions of oncogenes and tumor suppressors, which are deregulated during tumor progression.

1.2 EMT and cancer

"Epithelial-mesenchymal transition" (EMT), was first observed during the embryonic development (Savagner et al., 1994). Later it was shown that also cells in primary tumors undergo an EMT in order to invade and metastasize to distant organs (Thiery, 2002a). During EMT transformed epithelial cells can acquire the abilities for tumor invasion and metastasis, to resist apoptosis, and to disseminate (De Craene and Berx, 2013). Numerous laboratories demonstrated that EMT can be activated by a group of factors, SNAIL1, SNAIL2, Vimentin (VIM), ZEB1, ZEB2, ZNF281 and AP4, and repressed by CDH1 (Gregory et al., 2008; Hahn et al., 2013; Jackstadt et al., 2013; Siemens et al., 2011). Another important EMT regulator is transforming growth factor β (TGF-β). It up-regulates SNAIL1 and SNAIL2 and is an inducer of EMT in cancer cells (Siemens et al., 2011). As non-coding RNAs were reported to play

an important role in cancer metastasis, they are also potential hallmarks of the EMT program. For example, the miR-34/SNAIL1 and miR-200/ZEB1/2 pathways. The members of the miR-34 family directly repress SNAIL1 and miR-200 members repress ZEB1/2, both promoting mesenchymal-epithelial transition (MET) (Gregory et al., 2008; Siemens et al., 2011).

Cells undergoing an EMT also acquire other traits important for cancer cells. For example, they acquire features of cancer stem cells (CSCs). For example, elevated expression of β-catenin, a central component of Wnt and stem cell signaling, was found at the invasive front of the primary tumor in cells expressing EMT markers (Arend et al., 2013; Fodde and Brabletz, 2007). Stem-like cells in normal mammary glands and breast tumors also express EMT-related markers (Mani et al., 2008).

A **B**

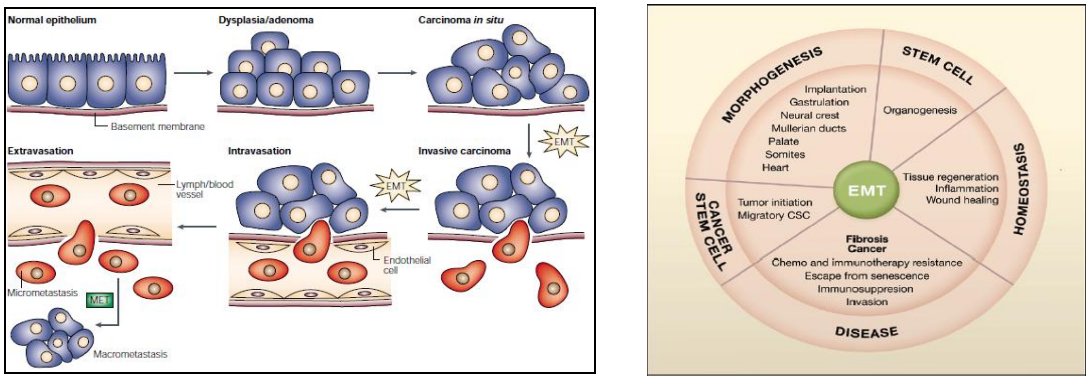

Figure 2 EMT processes and multiple crossroads

(A) Role of EMT and MET in the progression of tumors. Normal epithelia give rise to adenomas which locally grow within the borders of a basement membrane. Additional transformation by epigenetic changes and genetic alterations leads to a carcinoma *in situ*, still surrounded by an intact basement membrane. Further changes can induce EMT which promotes local dissemination of carcinoma cells and invasion into and beyond the basement membrane. Thereby cells can intravasate into lymph or blood vessels, allowing their passive transport to distant organs (micrometastasis) or they can form a new carcinoma through MET (Thiery, 2002a). At secondary sites, solitary carcinoma cells can extravasate. Figure adapted to Thiery, 2002. (B) Involvement of EMT in multiple cellular processes (Thiery et al., 2009). Figure adapted to Thiery, 2009.

1.3 The biology of colorectal cancer

Colorectal cancer arises due to the accumulation of genetic and epigenetic changes, which transform normal glandular epithelial cells into invasive adenocarcinomas. In the past decades, intensive research identified two major different molecular mechanisms as the cause of colorectal cancer: chromosomal instability (CIN) and microsatellite instability (MSI) (Al-Sohaily et al., 2012; Fearon and Vogelstein, 1990). CRC with CIN represent 80% of sporadic CRC and is characterized by allelic losses on the short arm of chromosome 17 and 8 and on the long arm of chromosome 5, 18 and 22. These allelic losses are linked to mutations in *TP53*, *APC*, *SMAD2* and *SMAD4* genes (Rustgi, 2013). It is still controversial how the CIN phenotype is generated. Hadjihannas *et al* claimed that aberrant Wnt/beta-catenin signaling results in CIN (He et al., 2007). Activated Wnt/beta-catenin signaling induces the transcription of target genes, including *conductin/AXIN2*, which also binds to polo-like kinase 1. This may compromise the spindle checkpoint, which suppresses chromosomal instability (Hadjihannas et al., 2006). On the other hand, MSI, which results from a mismatch repair (MMR) deficiency is present in 12-15% of CRC cases. MMR deficiency leads to the accumulation of mutations in genes, such as *TGFBRII*, *BAX* or *CASPASE5*, which regulate the cell cycle and apoptosis (Fleming et al., 2013; Lee et al., 2013). CRC shows genetic heterogeneity as shown above, but the consequences of signaling pathway alterations are similar. For example, the RAS-MAP kinase pathway is triggered by KRAS mutations in CIN tumors or by BRAF mutations in MSI tumors. The p53 pathway is inactivated by TP53 inactivation due to mutations and deletions in CIN and MSI tumors or, alternatively, by BAX inactivating mutations in MSI tumors (Friedman et al., 2009; Laurent-Puig et al., 2010).

1.4 p53

p53 is presumably the best studied tumor suppressor. Inactivation of p53 is observed in 50% of all human cancers (Hollstein et al., 1991). p53 and its numerous target genes play an essential role in suppressing many human tumors (Levine et al., 2004; Vousden and Prives, 2009).

1.4.1 p53 enters the microRNA world

miRNAs play a role in the regulation of proliferation, differentiation and apoptosis, and are intimately connected to the p53 network (Hermeking, 2012, Nature Reviews Cancer). Several groups documented that p53 induces the expression of several miRNAs and promotes the maturation of specific miRNAs, which mediate tumor suppression by p53 (Kim et al., 2011b; Shimono et al., 2009; Xu et al., 2009). Some laboratories reported that p53 inhibits cell proliferation and tumor angiogenesis through miR-107 (Chen et al., 2013a; Corney et al., 2007). The *miR-34* family includes the *miR-34a* and *miR-34b/c* genes, which were the first miRNAs found to be directly regulated by p53. Activation of p53 induces miR-34, which represses the EMT-induced transcription factor *SNAIL* (Siemens et al., 2011). Similarly, the p53-induced *miR-200* family represses the EMT-TFs ZEB1/ZEB2, thereby forming a double-negative feed-back loop (Chang et al., 2011).

1.5 microRNAs and cancer

As the name implies, microRNAs (miRNAs) are short, single-stranded RNAs of ~22 nucleotides length. They constitute a relatively new class of gene regulators in plants and animals (Bartel, 2004). The earliest description of miRNAs can be found in *Caenorhabditis elegans,* where they function as

regulators of developmental timing (Lee et al., 1993; Wightman et al., 1993). To date, approximately 2500 miRNAs have been identified in humans. miRNAs are known to modulate the stability of the mRNA targets through 3'-untranslated regions (3'-UTR). Over 60% of all mammalian mRNAs are predicted to be targets of miRNAs (Friedman et al., 2009). miRNAs are involved in many processes, such as development, stem cell division, apoptosis, disease and cancer (Cheng et al., 2005a; Cheng et al., 2005b; Cimmino et al., 2005).

1.5.1 The biogenesis of miRNAs

miRNAs are generated by a unique biogenesis, which is closely related to their regulatory functions (Bartel, 2004). As shown in Figure 3, they are encoded by specific host genes in genomic DNA, which are transcribed by RNA polymerase II to yield the primary transcript (pri-miRNA) containing a stem-loop structure of ~500 to 3,000 bp. pri-miRNAs are capped and polyadenylated and possess hairpin structures that comprise the future mature sequence in the stem. These pri-miRNAs in the nucleus are further transformed into ~60-70 nt hairpin-shaped precursor miRNAs (pre-miRNAs) by the Drosha enzyme, a type III RNase, in a complex with its co-factor DGR8 (DiGeorge syndrome critical region 8 homolog) (Han et al., 2006). The pre-miRNAs are exported into the cytoplasm by the RAN GTP-dependent transporter Exportin-5 (Exp-5) (Lund et al., 2004). After being transported into the cytoplasm, the pre-miRNA hairpin is cleaved by Dicer (RNase III) and with assistance of TRBP (TAR RNA-binding protein, also known as TARBP2) a ~22 nt RNA duplex is generated (Chendrimada et al., 2005). One of the two strands, the so-called passenger strand (miRNA*), is released and degraded. Another strand which is termed guide strand or miRNA, is loaded into the Argonaute-containing RNA-induced silencing complex (RISC). miRNA-RISC

complexes are able to silence the target mRNAs via imperfect complementarity with target sequences located most commonly in the 3'-UTR. (Esquela-Kerscher and Slack, 2006; Lujambio and Lowe, 2012; Ruegger and Grosshans, 2012).

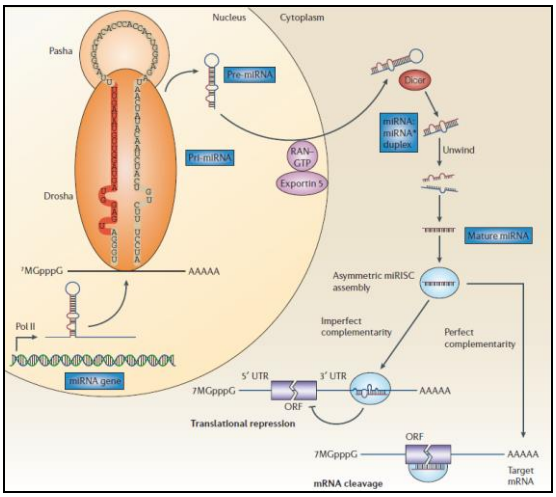

Figure 3 The biogenesis of microRNAs

MicroRNAs (miRNAs) are mainly transcribed by RNA Polymerase II (Pol II) in the nucleus to synthesize a primary transcript called pri-miRNA. Then, the pri-miRNA transcript is processed by the RNase III enzyme Drosha to release a~70-nucleotide pre-miRNA precursor product named pre-miRNA. RAN-GTP and exportin 5 transport the pre-miRNA into the cytoplasm. Subsequently, another RNase III enzyme, Dicer, processes the pre-miRNA to generate a transient ~22-nucleotide miRNA in conjunction with TRBP. One of the two strands, named miRNA, is then loaded into the miRNA-associated RNA-induced silencing complex (miR-RISC), which includes the Argonaute protein, and mature single-stranded miRNA. Then, mature miRNA binds to complementary sites in the 3'-UTRs of target mRNA genes and regulates gene expression (Esquela-Kerscher and Slack, 2006). Figure adapted to Esquela-Kerscher and Slack, 2006.

1.5.2 miRNAs and diseases

Recently, microRNAs have attracted a lot of attention because of their functions in human diseases. miRNAs have been identified as important regulators in a variety of biological processes including embryogenesis,

differentiation, proliferation, apoptosis, signal transduction and carcinogenesis. Abnormal expression of miRNAs is involved in the pathogenesis of human diseases including cancer, hematopoietic diseases and viral infection.

1.5.3 miRNAs and cancer

The first genetic proof of a role of miRNAs in human cancers was obtained in 2002. Croce and colleagues observed that a small genomic region located on chromosome 13q14 is commonly deleted in chronic lymphocytic leukemia (CLL). Since the region contains the *DLEU2* gene which encodes *miR-15a/16-1* this finding suggests a link between these miRNAs and CLL (Calin et al., 2002). Moreover, 52.8% (98 of 186) of annotated human miRNAs locate in the fragile sites, which are linked to cancer (Calin et al., 2004). This indicates that miRNAs may have a crucial function in cancer progression. For example, miR-125b maps to the fragile site of chromosome 11q24, which is deleted in a subset of breast, lung, ovarian and cervical cancers (Feliciano et al., 2013; Gong et al., 2013). That suggested that miR-125b functions as a tumor suppressor in these cancer types. On the other hand, certain miRNAs exhibit oncogenic properties. For instance, miR-21 was found to stimulate cell invasion and metastasis in different tumor types such as breast cancer, colon cancer and glioma (Asangani et al., 2008; Gabriely et al., 2008; Zhu et al., 2008). Several examples of miRNAs that are aberrantly expressed in cancer and function either a tumor suppressor or as oncogenes are summarized in Table I.

Table I The functions of miRNAs as oncogenes or tumor suppressors in cancer.

miRNA	Genomic location	Cancer type	Targets	Mechanism
Oncogenes				
miR-21	17q23.1	colon, breast, lung, liver, stomach cancer	*PTEN, TPM1*	anti-apoptotic factor, EMT, cancer stem cell phenotype
miR-155	21q21.3	lung and breast cancer, AML, Hodgkin lymphoma	*c-maf, SHIP1*	Wnt signaling, tumor metastasis, cell proliferation, NF-kB
miR-17~92	13q22	breast, lung and colon cancer neuroblastoma, CLL	*E2F1, Bim, PTEN STAT5, Nanog*	apoptosis, stemness
miR-373	19q13	testicular, breast, liver, prostate cancer	*CD44, TNFAIP1 RAD23B*	invasion/metastasis, stemness, TGF-β signaling, hypoxia-inducible
miR-10b	2q31	breast, ovarian, gastric, bladder, malignant glioma	*HOXD10, TBX5 Tiam1, MAPRE1*	TGF-β signaling, EMT, cell motility, cell proliferation, hypoxia-inducible
miR-221/222	Xp11.3	lung, hepatocellular carcinoma, Invasive ductal carcinoma	*PTEN, HECTD2, KIT, RAB1A*	cell proliferation/apoptosis, JAK/STAT signaling

Tumor suppressors				
miR-15a/16-1	13q14	CCL, BCL, colon and breast cancer	*BCL2, CCND1, VEGF, AP4,WT-1*	frequently deleted, apoptosis, decreases tumorigenicity, EMT
miR-143/145	5q32	colon, breast, prostate, lung, lymphoid cancer	*Osx, KLF4 GOLM1*	Toll-like receptor signaling, stemness, cell proliferation, migration/invasion
let-7 family		lung, breast and ovarian cancer	*RAS, c-MYC, ITGB3, HMGA2*	apoptosis, Wnt signaling, cell proliferation, Lin28-Let-7 axis
miR-29	7q32 and 1q30	CLL, AML, lung and breast cancer	*TCL-1, MCL1, DNMT3a*	apoptosis, decreases tumorigenicity TGF-β signaling
miR-34 Family	1p36 and11q23	breast, kidney, colon and lung cancer	*SNAIL1, c-MYC, ZNF281*	induces apoptosis, EMT, apoptosis, decreases tumorigenicity, stemness
miR-200 Family	1p36	colon, breast and prostate cancer	*ZEB1/2, CCNE2, FLT1, VEGF*	EMT, stemness, cell cycle, angiogenesis
miR-101	1p31.3	prostate, breast, ovarian, lung and colon cancer	*EZH2, NLK, ZEB1/2, c-MET*	cell proliferation, EMT
miR-26a	3p22	liver, ovarian cancer	*CCND2, CCNE2 HMGA1, LIN28B*	cell proliferation and motility, NF-kB signaling

Abbreviations: *BCL2*, B-cell CLL/lymphoma 2; *Bim*, BCL-2-interacting mediator of cell death; CLL, chronic lymphocytic leukemia; *CCND2*, cyclin D2; *CCNE2*, cyclin E2; *c-MET*, c-MET proto-oncogene; *DNMT3a*, DNA (cytosine-5-)-methyltransferase 3 alpha; ECM, extracellular matrix; *EZH2*, enhancer of zeste 2 polycomb repressive complex 2 subunit; EMT, epithelial-mesenchymal transition; *E2F1*, E2F transcription factor 1; *FLT1*, fms-related tyrosine kinase 1; *GOLM1,* golgi membrane protein 1; *HOXD10*, homeobox D10; *HMGA1/2*, high mobility group AT-hook 1/2; *ITGB3*, integrin, beta 3; *LIN28B*, lin-28 homolog B; *maf*, v-maf avian musculoaponeurotic fibrosarcoma oncogene homolog; *MCL1*, myeloid cell leukemia sequence 1; *MYC*, v-myc avian myelocytomatosis viral oncogene homolog; NF-kB, nuclear factor-kB; *Osx,* Osterix*; NLK,* Nemo-like kinase*; PTEN*, phosphatase and tensin homolog; *SHIP1*, Phosphatidylinositol-3,4,5-trisphosphate 5-phosphatase 1; *SNAIL1*, snail family zinc finger 1; *TCL-1*, T-cell leukemia/lymphoma 1; *TPM1*, tropomyosin 1; *VEGF*, vascular endothelial growth factor; *ZEB1/2*, zinc finger E-box binding homeobox *1/2*; *ZNF281,* zinc finger protein 281.

1.6 The miR-15a/16-1 family

The deregulation of many miRNAs observed in cancer suggests that they may be causally involved in the initiation or progression of cancer. Calin *et al* showed that miR-15a/16-1 is involved in CLL, the most common form of adult leukemia in the Western world (Calin et al., 2002). Chiorazzi*et al.* found that *DLEU2*, the host gene of miR-15a and miR-16-1, is deleted in half of CLL cases (Chiorazzi et al., 2005). This suggested that the two miRNAs could be the tumor suppressor genes.

Several studies have shown that miR-15a and miR-16-1 are deleted or down-regulated in tumor cells, suggesting that these two miRNA genes could be the “hot spots” in cancer transformation (Bonci et al., 2008; Calin and Croce, 2006). Moreover, Cimmino *et al* found that miR-15a/16-1 induces apoptosis by targeting the oncogene *BCL2*. They noted that the expression of miR-15a and miR-16-1 inversely correlates with *BCL2* expression in CLL and miR-15a/16-1 represses *BCL2* at the post-transcriptional level (Cimmino et al., 2005).

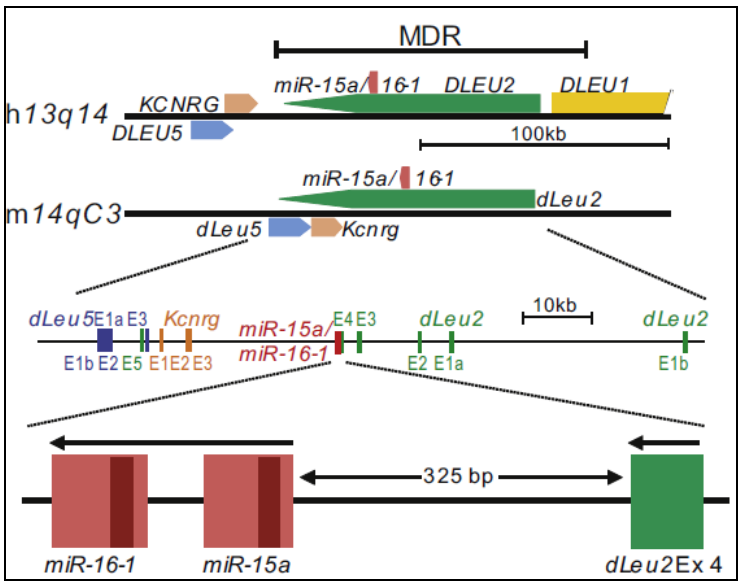

Figure 4 *DLEU2* is the host gene of miR-15a and miR-16-1

Schematic figures present the human 13q14 and mouse 14qC3. Thick arrows show the 5'-3' orientation. MDR, minimal deleted region (Klein et al., 2010). Figure adapted to Klein et al., 2010.

1.7 The transcription factor AP4

The AP4/TFAP4 (Transcription factor AP4) protein activates both viral and cellular genes by binding to the symmetrical DNA sequence, CAGCTG. The AP4 is a basic helix-loop-helix (bHLH) protein (Hu et al., 1990). It was identified first as a cellular protein that binds to the SV40 enhancer and interacts synergistically with AP-1 to activate viral late gene transcription (Mermod et al., 1988). Unlike other bHLH transcription factors, AP4 contains two additional protein dimerization motifs, which consist of the leucine zipper elements LZ1 and LZ2 (Jung and Hermeking, 2009).

AP4 was shown to play an important role in modulation of cellular functions, such as viral production (Imai and Okamoto, 2006), cell growth and survival (Tsujimoto et al., 2005), immune response (Aranburu et al., 2001; Bae et al., 2001), and angiogenesis (Cui et al., 1998) by regulation of specific target genes.

Recently, the *AP4* gene was characterized as a *c-MYC* target gene and its product was shown to repress *p21* in order to maintain cells in a proliferative, progenitor-like state (Jung and Hermeking, 2009; Jung et al., 2008). Furthermore, Jackstadt *et al* revealed that ectopic expression of AP4 induces EMT by regulating a specific set of genes, such as *SNAIL*, *VIM*, and repressing *CDH1* expression in colorectal cancer (CRC) cells (Jackstadt et al., 2013). In accordance with these results, AP4 also enhances migration/invasion, whereas knock-down of AP4 decreases the formation of lung metastasis by CRC cell in mice (Jackstadt et al., 2013).

1.8 The transcription factor MYC

The MYC family comprises the transcription factors c-MYC, n-MYC, L-MYC, b-MYC and S-MYC, and performs essential functions during proliferation, growth, survival and differentiation of normal cells. MYC transcription factors belong to the class of basic region/helix-loop-helix/leucine zipper (bHLHZip) transcription factors and heterodimerize with Max, another bHLHZip protein. The MYC/MAX heterodimers binds to the 6-nucleotide DNA consensus sequence CACGTC, the so-called E-box (Luscher and Larsson, 1999).

The v-MYC oncogene was discovered in a retrovirus that causes myelocytomatosis (Duesberg and Vogt, 1979; Hu et al., 1979). The expression of n-MYC and L-MYC genes is largely confined to particular stages of the embryonic development and to immature cells of the hematopoietic and neuronal compartment of adults. In contrast, the c-MYC gene is expressed in dividing cells and is down-regulated during differentiation when cells stop to proliferate (Meyer and Penn, 2008). c-MYC expression is induced by multiple mitogenic signaling pathways including Wnt, Notch and STAT signaling, as well as by activation receptor tyrosine kinases (RTKs), such as PDGFR (platelet-derived growth factor receptor), EGFR (epidermal growth factor

receptor) and IGFR (insulin-like growth factor 1 receptor) (Bommer et al., 2007; Chang et al., 2007; Raver-Shapira et al., 2007).

As has been mentioned, MYC is crucial in normal cell proliferation and growth. However, deregulation of MYC gene can result in an enlarged pool of proliferating and self-renewing cells, which are more likely to acquire further mutations that accelerate tumorigenesis. Indeed, activation of the MYC oncogene, as a consequence of translocation, amplification, point mutations or defects in upstream regulators, contributes to the development of a wide variety of human cancers including leukemia, lymphoma and solid cancers, such as breast cancer and neuroblastoma (Aulmann et al., 2006; Bourhis et al., 1990). However, deregulation of MYC also triggers intrinsic tumor suppressor mechanisms including apoptosis, cellular senescence and DNA damage responses. These checkpoint responses constitute main barriers for tumor development (Liu et al., 2012). The seemingly antagonistic functions of MYC functions have been comprehensively reviewed recently (Larsson and Henriksson, 2010).

1.9 Aims of the Study

AP4 functions as an oncogene that regulates EMT and thereby mediates invasion and migration. The goal of this study was to identify miRNAs, which regulate AP4 and may thereby exert tumor suppressive functions.

2 Materials

2.1 Human cancer cell lines

Five colon cancer cell lines, one kidney cancer cell line and one lung cancer cell line which stored by our group were used in this study. The SW480 cell line was established from a 50 years old male patient of Dukes' type B, colorectal adenocarcinoma. The SW620 cell line was established from a 51 years old male patient of Dukes' type C, colorectal adenocarcinoma. The DLD1 cell line was established from a male patient of Dukes' type C, colorectal adenocarcinoma. The HCT116 cell line was established from a male patient of colorectal carcinoma. The RKO cell line was established from a patient of colorectal carcinoma. The kidney cell line HEK-293 was established from a fetus of the embryonic kidney. The lung cancer cell line H1299 was established from a 43 years old male patient of non-small cell lung cancer.

2.2 Chemicals

2.2.1 General chemicals

Name	Company
Ampicillin	Sigma-Aldrich, St. Louis, MD, USA
Christal violet	Carl Roth GmbH, Karlsruhe, Germany
DMEM (1×) GlutaMAX™–I	Life Technologies Corporation, Grand Island, NY, USA
DMSO	Carl Roth GmbH, Karlsruhe, Germany
Doxorubicin	Sigma-Aldrich, St. Louis, MD, USA
Doxycycline hyclate	Sigma-Aldrich, St. Louis, MD, USA
Ethanol	Carl Roth GmbH, Karlsruhe, Germany

Ethidium bromide	Carl Roth GmbH, Karlsruhe, Germany
FBS (fetal bovine serum)	Gibco®, Life Technologies Corporation, Grand Island, NY, USA
HBSS+/+, HBSS -/-	Life Technologies Corporation, Grand Island, NY, USA
Hygromycin B	Invitrogen GmbH, Karlsruhe, Germany
McCoy's 5A medium (1x)	Life Technologies Corporation, Grand Island, NY, USA
Methanol	Carl Roth GmbH, Karlsruhe, Germany
Penicillin/Streptomycin 100 ml	Life Technologies Corporation, Grand Island, NY, USA
Puromycin dihydrochloride	Sigma-Aldrich, St. Louis, MD, USA
Trypsin (10x, phenol-red free)	Invitrogen GmbH, Karlsruhe, Germany
Tween® 20	Sigma-Aldrich, St. Louis, MD, USA
Distilled Water	Life Technologies GmbH, Darmstadt, Germany

2.2.2 Cell culture materials

Name	**Company**
25 cm^2, 75 cm^2 , 150 cm^2, culture flask, Canted Neck	Corning Incorporated Corning, NY, USA
6-, 12-, 24-, and 96-well cell culture Cluster	Corning Incorporated Corning, NY, USA
Costar® STRIPETTE® 2 ml, 5 ml, 25 ml, 50 ml	Corning Incorporated Corning, NY, USA
Cell Culture Dish 60 mm×15 mm and 100 mm×20 mm style	Corning Incorporated Corning, NY, USA

2.2.3 Cell culture medium

Cell line	Medium
SW480/SW620/H1299	90% DMEM medium
cell lines medium	10% FBS
	1% Penicillin/Streptomycin
HCT 116/RKO/DLD1	90% McCoy’s medium
cell lines medium	10% FBS
	1% Penicillin/Streptomycin

2.2.4 Cell storage medium

Component	Percentage
DMEM/McCoy’s medium	40%
FBS	50%
DMSO	10%

2.2.5 Vectors

Name	Insert	Reference
pRTR		(Jackstadt et al., 2013)
pRTR-p53-VSV	human p53	(Siemens et al., 2011)
pRTR-AP4-VSV	human AP4	(Jackstadt et al., 2013)
pRTS-miR-15a/16-1	human miR-15a/16-1	(Klein et al., 2010)
TW empty		(Bonci et al., 2008)
TW-miR-15a/16-1	human miR-15a/-16-1	(Bonci et al., 2008)
TW-miR-15a/16-1 sponge	human miR-15a/-16-1	(Bonci et al., 2008)
pGL3-control-MCS		
pGL3-AP4 3'-UTR	human *AP4* 3'-UTR	(Shi et al., 2014)
pGL3-AP4 3'-UTR MUT	human *AP4* 3'-UTR MUT	(Shi et al., 2014)
pRL	Renilla	

2.2.6 Materials for transfection and real time PCR

Name	Company
Fast SYBR® Green Master Mix	Applied Biosystems, Foster City, CA,
FuGene® 6 Transfection reagent	Promega, Madison, WI, USA
HiPerFect Transfection reagent	Qiagen GmbH, Hilden, Germany
Lipofectamine® 2000	Invitrogen GmbH, Van Allen Way CA, USA
Opti-MEM®	Life Technologies Corporation, Grand NY, USA
DNase I (RNase-free)	Sigma-Aldrich, St. Louis, MD, USA
High Pure miRNA Isolation Kit	Roche Diagnostics GmbH, Mannheim,

	Germany
High Pure RNA Isolation Kit	Roche Diagnostics GmbH, Mannheim, Germany
Verso cDNA Kit	Thermo Fisher Scientific Inc., Waltham, USA
miRCURY LNA™ Universal RT microRNA PCR, Universal cDNA Synthesis Kit II, 8-64 xns	Exiqon A/S, Vedbaek, Denmark
miRCURY LNA™ Universal RT microRNA PCR, SYBR® Green master mix, universal RT, 2.5 ml	Exiqon A/S, Vedbaek, Denmark

2.2.7 Materials for Western blot, flow cytometry and immunofluorescence

Name	**Company**
0.22 µm filter (Millex®-GV)	Merck Millipore Ltd. Tullgreen, Carrigwohill, Co. Cork, IRL
APS	Carl Roth GmbH, Karlsruhe, Germany
β-mecaptoethanol	Sigma-Aldrich Chemie GmbH, Steinheim, Germany
Complete mini protease inhibitor cocktail	Roche Diagnostics GmbH, Mannheim, Germany
DAPI	Carl Roth GmbH, Karlsruhe, Germany
Immobilon^{TM} Western	Millipore Corporation, Billerica, MA, USA
Immobilon-P Transfer Membrane	Immobilon, Merck Millipore, Billerica, MA, USA
Micro BCA Protein Assay Kit	Pierce, Thermo Fisher Scientific, Inc.,

	Rockford, IL, USA
NaCl	Carl Roth GmbH, Karlsruhe, Germany
Nonidet® P40 Substitute	Sigma-Aldrich, St. Louis, MD, USA
PageRuler™	Thermo Fisher Scientific, Inc.,
Prestained Protein Ladder	Rockford, IL, USA
Paraformaldehyde	Merck KGaA, Darmstadt, Germany
ProLong Gold Antifade	Invitrogen GmbH, Karlsruhe, Germany
Propidium iodide	Sigma-Aldrich, St. Louis, MD, USA
RNase A	Sigma-Aldrich, St. Louis, MD, USA
Rotiphorese Gel 30 (37, 5:1)	Carl Roth GmbH, Karlsruhe,
	Germany
SDS (sodium dodecyl sulfate)	Carl Roth GmbH, Karlsruhe, Germany
Skim Milk Powder	Fluka, Sigma-Aldrich, St. Louis, MD,
	USA
Tris-base	Carl Roth GmbH, Karlsruhe, Germany
Triton X 100	Carl Roth GmbH, Karlsruhe, Germany
TEMED	Carl Roth GmbH, Karlsruhe, Germany
Western Lighting^{TM} Plus-ECL	Millipore Corporation, Billerica,
	MA, USA

RIPA buffer (for protein lysates, 100 ml):

- 1% NP40
- 0.5% sodium deoxycholate
- 0.1% SDS
- NaCl 150 mM
- 50 mM TrisHCl (pH 8.0)

2xLaemmli buffer (9 ml):

- 1 ml, 125 mM TrisHCl (pH 6.8)
- 4 ml, 10% SDS
- 2 ml, 20% glycerol
- 1 ml, 0.5% bromophenol blue (in H_2O)
- 1 ml ddH_2O
- 10% β-mercaptoethanol, added immediately before use

10xTris-glycine-SDS running buffer (5 L, for protein gels):

- 720 g glycine
- 150 g Tris base
- 50 g SDS
- pH 8.3-8.7
- add ddH_2O to 5 liters

Towbin buffer (for protein blotting, 1 L, 10×):

- 30.28 g glycine
- 144.14 g Tris-base
- ddH_2O (pH 8.6)

Towbin buffer (for protein blotting, 1×):

- 10%, 10×Towbin Buffer
- 20% methanol
- 70% ddH_2O

10xTBST (5 L):

- 500 ml 1M Tris (pH 8.0)
- 438.3 g NaCl
- 50 ml Tween 20
- add ddH_2O to 5 liters

Resolving gel, 10%, 10 ml:

H_2O	4.12 ml
4xLower Tris	2.5 ml
30% PAA37.5/1	3.33 ml
10% APS	0.075 ml
TEMED	0.0075 ml

Stacking gel, 4 ml:

H_2O	2.45 ml
4x Upper Tris	1 ml
30% PAA37.5/1	0.67 ml
10% APS	0.005 ml
TEMED	0.0075 ml

Propidium iodide staining solution (PI):

- 800 µl propidiumiodide (1.5 mg/ml)
- 1000 µl RNase A (10 mg/ml)
- 20 ml PBS 0.1% Triton X 100

Storage at 4°C in dark.

Staining solution (20 ml):

- PBS 18.1 ml
- Triton X 100 100 µl
- RNase 1000 µl
- PI 800 µl

The solution was passed through a 0.22 µm filter before use.

2.2.8 Materials for migration, invasion and would healing

Name	Company
BD Matrigel™	BD Bioscience, Heidelberg, Germany
Boyden chamber transwell	Corning Inc., Corning, NY, USA
IBIDI chamber	IBIDI GmbH, Munich, Germany
Mitomycin C	Sigma-Aldrich, St. Louis, MD, USA

2.2.9 Materials for cloning and dual-reporter luciferase assays

Name	Company
dNTPs	Thermo Fisher Scientific Inc., Waltham, MA, USA
Gene Ruler 100 bp plus DNA ladder	Fermentas GmbH, St. Leon-Rot, Germany
Hi-Di™ Formamide	Applied Biosystems, Foster City, CA, USA
FIREPol® DNA polymerase	Solis BioDyne, Tartu, Estonia
Platinum® Taq DNA polymerase	Invitrogen GmbH, Karlsruhe, Germany
Restriction endonucleases	New England Biolabs GmbH, Frankfurt, Germany
T4 DNA ligase	Thermo Fisher Scientific Inc., Waltham, MA, USA
DyeEx® 2.0 Spin Kit	Qiagen GmbH, Hilden, Germany
Pure Yield™ Plasmid Midiprep	Promega GmbH, Mannheim, Germany
QIAprep Spin Miniprep Kit	Qiagen GmbH, Hilden, Germany
QIAquick Gel Extraction Kit	Qiagen GmbH, Hilden, Germany
QuikChange II XL Site-Directed Mutagenesis Kit	Stratagene, Agilent Technologies GmbH & Co. KG, Waldbronn, Germany
Dual-Luciferase® Reporter Assay System	Promega Corporation, WI, USA

Mini Prep buffer 1 (MP1):

- 50 mM Tris-HCl (pH 8)
- 10 mM EDTA
- 100 µg/ml RNase A

Mini Prep buffer 2 (MP2):

- 200 mM NaOH
- 1% SDS

Mini Prep buffer 3 (MP3):

- 3 M potassium acetate
- pH 5.5

2.2.10 Oligonucleotides used for cloning and site-directed mutagenesis

Name	Sequence(5’ - 3’)
AP4 3’-UTR WT Fwd	5’-ACTCCGAGGCCTCAGACAGTGAC-3’
AP4 3’-UTR WT Rev	5’-TGGAAGATGAGACCTGGAGGCAGAG-3’
AP4 3’-UTR Mutant Fwd	5’-TGCTTCTTGGTTGGGGTTTCCAGTAGCTG TGCCCCCCTCCCCCTT-3’
AP4 3’-UTR Mutant Rev	5’-AAGGGGGAGGGGGGCACAGCTACTGGAA ACCCCAACCAAGAAGCA-3’

2.2.11 Oligonucleotides used for qPCR analyses

Name	Sequence(5’ - 3’)
pri-miR-15a/16-1 Fwd	5’-GCAATTACAGTATTTTAAGAGATGAT-3’
pri-miR-15a/16-1 Rev	5’-CATACTCTACAGTTGTGTTTTAATGT-3’
AP4 Fwd	5’-GCAGGCAATCCAGCACAT-3’
AP4 Rev	5’-GGAGGCGGTGTCAGAGGT-3’
β-actin Fwd	5’-TGACATTAAGGAGAAGCTGTGCTAC-3’
β-actin Rev	5’-GAGTTGAAGGTAGTTTCGTGGATG-3’
SNAIL Fwd	5’-GCACATCCGAAGCCACAC-3’
SNAIL Rev	5’-GGAGAAGGTCCGAGCACA-3’
CDH1 Fwd	5’-CCCGGGACAACGTTTATTAC-3’
CDH1 Rev	5’-GCTGGCTCAAGTCAAAGTCC-3’
Vimentin Fwd	5’-TACAGGAAGCTGCTGGAAGG-3’
Vimentin Rev	5’-ACCAGAGGGAGTGAATCCAG-3’
ZEB1 Fwd	5’-TCAAAAGGAAGTCAATGGACAA-3’
ZEB1 Rev	5’-GTGCAGGAGGGACCTCTTTA-3’

2.2.12 Oligonucleotides used for qChIP analyses

Name	Sequence(5’- 3’)
DLEU EX 1A Fwd	5’-CATGCGTAAAAATGTCGGGAA-3’
DLEU EX 1A Rev	5’-GGTTATTCCTGTCCGCTAGATTGA-3’
DLEU EX 1B Fwd	5’-GCGCGCTGTGTACTTAGG-3’
DLEU EX 1B Rev	5’-CAACATTGCGAAAAGGAG-3’
AchR Fwd	5’-CCTTCATTGGGATCACCACG-3’
AchR Rev	5’-AGGAGATGAGTACCAGCAGGTTG-3’

2.2.13 Antibodies used for Western blot (WB) and immunofluorescence (IF) analysis

Primary Antibodies

Name	Ordering no.	Company	Application	Dilution	Source
AP4	040213	AbD Serotec	WB; IF	1:1000;1:50	mouse
E-cadherin	334000	Invitrogen	WB	1:1000	mouse
α-tubulin	T-9026	Sigma	WB	1:1000	mouse
SNAIL	3879S	Cell Signaling	IF	1:100	rabbit
VSV	V4888	Sigma	WB	1:7500	rabbit
p53	SC-126	Santa Cruz	WB	1:1000	mouse
ZEB1	SC-25388	Santa Cruz	WB	1:1000	rabbit

Secondary Antibodies

Name/Conjugate	Ordering no.	Company	Application	Dilution	Source
anti-mouse/HRP	# W4021	Promega	WB	1:10,000	goat
anti-rabbit/HRP	# A0545	Sigma	WB	1:10,000	goat
anti-mouse/Alexa	# A21422	Invitrogen	IF	1:500	goat
anti-rabbit/Cy3	#715-165-150	Jackson Imm. Research	IF	1:500	donkey

2.3 Materials for animal experiments

Name	Source
immunodeficient NOD/SCID mice	Jackson Laboratory

2.4 Colon cancer samples

The colon cancer RNA sample collection and its analysis for AP4 protein expression was described previously (Jackstadt et al., 2013). In brief, formalin fixed-, paraffin embedded (FFPE) colon cancer samples from 94 patients that underwent surgical tumor resection at the Ludwig-Maximilians-Universität München between 1994 and 2005 were obtained from the archives of the Institute of Pathology. All tumors were located on the right side of the colon. The study was performed according to the recommendations of the local ethics committee of the Medical Faculty of the Ludwig-Maximilians-Universität München (Shi et al., 2014; Siemens et al., 2013).

2.5 Equipment

Device	**Company**
5417C table-top centrifuge	Eppendorf AG, Hamburg, Germany
ABI 3130 genetic analyzer capillary sequencer	Applied Biosystems, Foster City, USA
Accu-Jet Pro Pipette	BrandTech Scientific, Essex, CT, USA
Axiovert 25 microscope	Carl Zeiss GmbH, Oberkochen, Germany
BD Accuri™ C6 Flow Cytometer Instrument	Accuri, Erembodegem, Belgium
Biofuge *fresco*	Heraeus; Thermo Fisher Scientific, Inc., Waltham, MA, USA
Biofuge *pico* table top centrifuge	Heraeus; Thermo Fisher Scientific, Inc., Waltham, MA, USA
CF40 Imager	Kodak, Rochester, New York, USA

Fisherbrand FT-20E/365transilluminator	Fisher Scientific GmbH, Schwerte, Germany
Forma scientific CO_2 water jacketed incubator	Thermo Fisher Scientific, Inc., Waltham, MA, USA
GeneAmp® PCR System 9700	Applied Biosystems, Foster City, USA
Herasafe KS class II safety cabinet	Thermo Fisher Scientific, Inc., Waltham, MA, USA
HTU SONI130 Labortechnik	G. Heinemann Ultraschall und Schwäbisch Gmünd, Germany
ME2CNT membrane pump	Vacuubrand GmbH & CO KG, Wertheim, Germany
Megafuge 1.0R	Heraeus; Thermo Fisher Scientific, Inc., Waltham, MA, USA
Mini-PROTEAN®-electrophoresis	Bio-Rad, Munich, Germany
MultiImage Light Cabinet	Alpha Innotech, Johannesburg, South Africa
Nalgene Cryo1°C Freezing Container	Thermo Fisher Scientific Inc., Waltham, MA, USA
ND 1000 NanoDrop Spectrophotometer	NanoDrop products, Wilmington, DE, USA
Neubauer counting chamber	Carl Roth GmbH & Co, Karlsruhe, Germany
Orion II illuminometer	Berthold Technologies GmbH & Co. KG, Bad Wildbad, Germany
PerfectBlue™ SEDEC 'Semi-Dry' blotting system	Peqlab Biotechnologie GmbH, Erlangen, Germany
Water bath	Memmert GmbH, Schwabach, Germany

3 Methods

3.1 Cell culture

3.1.1 Starting cell culture from frozen cells

Frozen cells were thawed in a 37°C water bath. Afterwards cells were transferred into a 15 ml falcon, centrifuged at 1200 rpm for 4 minutes. The cell pellet was washed the first time with HBSS-/- (Life Technologies), re-centrifuged, washed the second time with appropriate medium (see 2.2.3), then transferred into a flask. Cells were cultivated in an incubator at 37°C and 5% CO_2.

3.1.2 Subculture of adherent cell lines

Cell culture was watched using an inverted microscope to check confluence and confirm the absence of contaminants. The used medium was removed. The cell monolayer was washed with HBSS. 1×trypsin (1-2 ml per T75 flask) was added to the washed cell monolayer. The flask was kept in an incubator at 37°C for 3-5 minutes or until cells were detached. After that, the flask was gently taped to release the adherent cells. Detachment was checked with a microscope. Cells were splitted and fresh serum-containing medium was added. Cells were cultivated in an incubator at 37°C and 5% of CO_2.

3.1.3 Cell counting

Cells were detached from the surface of the dish by using trypsin and diluted with medium. A sterile pipet tip was used to transfer the cell suspension to the edge of Neubauer counting chamber (Roth). Cells were allowed to settle for a

few minutes before counting. The slide was viewed on a microscope with 10×magnifications. A hand-held counter was used to count cells in each of four corner squares. The cell concentration can be determined with the following formula: cells/ml= total number of 4 corners×10^4/4.

Coverslip and Neubauer counter chamber were rinsed with 70% ethanol.

3.1.4 Cell storage

Cells were trypsinized, centrifuged at 1200 rpm for 4 minutes and resuspended in storage medium. Aliquots in cryovials were stored in cell freezing container (Thermo Fisher Scientific) at -80°C for up to six months or in liquid nitrogen tank for long term storage.

3.1.5 Transfection of oligonucleotides, vectors and constructs

Most of the transfection experiments were performed in 6-well plates.

1.0-4.0 × 10^5 cells per well were seeded in 2 ml medium. For each well, the transfection mixture contained 150 µl Opti-MEM (Life Technologies), 5 µl oligonucleotides (10 µM) or 4 µg DNA constructs and 10 µl HiPerFect (Qiagen) or 8µl FuGene reagent (Promega). The mixture was gently mixed by vortexing and incubated at room temperature for 10 minutes (for oligonucleotides) or 15 minutes (for DNA constructs), then it was added dropwise to the cells, incubated for 24 - 48 hours until the cells were ready for the assay.

3.1.6 Generation of cell pools with conditional vectors

DLD-1 and SW480 colorectal cancer cells were transfected with pRTR or pRTS plasmids using FuGene reagents. After 24 hours, cells were transferred into media containing 4 µg/ml puromycin (Sigma; stock solution: 2 mg/ml in water) for one week or into media containing 800 µg/ml hygromycin (Invitrogen; stock solution 50 mg/ml) for two weeks. Homogeneity of the derived cell pools was tested by addition of 100 ng/ml DOX for 48 hours. After that GFP/RFP expression was evaluated by fluorescence microscopy and flow cytometry (Shi et al., 2014).

3.2 Generation of the *AP4* 3'-UTR constructs

3.2.1 Clone the *AP4* 3'-UTR constructs

The *AP4* 3'-UTR fragment containing the *miR-15a/16-1* seed sequence was amplified by PCR using of the primers listed above (see 2.2.10) and inserted into the AgeI and EcoRV sites of the multiple cloning site of the pGL-3 vector**.** The reagents were: 2 µl 10×PCR buffer,1.2 µl dNTPs, 1.6 µl Fwd primer,1.6 µl Rev primer, 2 µl template (100 ng), 0.3 µl Hot Star, 1 µl DMSO and 10.3 µl ddH_2O. The PCR program started at 94°C for 10 min for initial activation, 3-step 35×cycling of 94°C for 1 min for denaturation, 56°C for 1 min for annealing and 72°C for 1 min for extension, then the final extension at 72°C for 7 min. PCR results were detected by gel electrophoresis with a 1% agarose gel.

Mutations of the *miR-15a/16-1* seed-matches were introduced using the QuickChange II Site-Directed Mutagenesis Kit (Stratagene) with oligonucleotides listed above (see 2.2.10) and confirmed by sequencing.

3.2.2 Colony PCR

To identify the inserted positive transformants, a bacterial culture tube containing selective medium was prepared. In parall, 20 µl PCR reaction mixture containing dNTPs, PCR buffer, vector-specific primers, and FIREPol® DNA polymerase was prepared. A single colony was picked from the bacterial culture and transferred into the PCR reaction and thereafter inoculated in the culture tube overnight.

PCR cycling conditions were as follows: 95°C for 5 minutes initial activation, followed by 25 cycles. Denaturation at 95°C for 30 seconds, annealing at 62°C for 30 seconds and 72°C for 1 minute or longer for extension, depending on the size of insert, and then 72°C for 2 minutes. PCR results were detected by gel electrophoresis with a 1% agarose gel.

3.2.3 Ligation method

The ligation mixture containing 3 µl PCR product (15 ng), 1 µl pGEM-T-Easy vector (5 ng), 1 µl 10×ligation buffer, 1 µl T4 DNA Ligase and 4 µl ddH_2O, was gently mixed and placed overnight at 4°C.

3.2.4 Transformation of heat shock-competent *E. Coli* XL1 blue

Competent *E. coli* XL1 blue cells were thawed on ice for ~30 minutes and agar plates (containing the appropriate antibiotic) were kept at room temperature or in a 37°C incubator. The water bath was kept at 42°C. 100 ng plasmid was added to 25 µl of competent cells in a micro-centrifuge tube, gently mixed and incubated on ice for 30 minutes. Subsequently, each transformation tube was kept in the 42°C water bath for 90 seconds for heat shock and put back immediately on ice for 2 minutes. 500 µl LB medium

(without antibiotics) was added and the mixture was kept in the 37°C incubator for 60 minutes. Cells were centrifuged at 2000 rpm for 5 minutes, the major part of the supernatant was discarded. The remaining cells were plated on an agar plate containing antibiotics. A bent one-way inoculation needle was used to spread them as equally as possible. Finally, the plate was incubated upside-down at 37°C over night.

3.2.5 Purification of plasmid DNA from *E.coli*

For miniprep of plasmid DNA, bacteria were inoculated in a volume of 5 ml of LB-medium supplemented with ampicillin. DNA was either isolated using the QIAprep Spin Miniprep Kit (Qiagen) as follows:

First, cells were centrifuged for 10 minutes at 4000 rpm. The pellet was resuspended in 250 µl of MP1 buffer, 250 µl of MP2 buffer and then incubated at room temperature for 5 minutes. The lysis buffer was neutralized by 250 µl of MP3 buffer and then centrifuged at 13000 rpm for 10 minutes. Subsequently, supernatant was transferred into a new tube, 700 µl of isopropanol was added and the mixtures were vortexed. Precipitated DNA was centrifuged at maximum speed for 15 minutes at room temperature, washed with 500 µl of 70% ethanol and centrifuged again at maximum speed for 5 minutes. After discarding the ethanol, DNA was dried at room temperature and resuspended in 50 µl H_2O.

For midi-prep, the volume of LB-medium was 150 ml and the Pure Yield™ Plasmid Midiprep System (Promega) was utilized according to the manufacturer's protocol.

3.2.6 Sequencing

The following regents were mixed in a sterile tube: 1 µl Big Dye Terminator 3V1.1 (Life Technologies), 2 µl 5×Sequencing buffer, 0.5 µl primer (10 µM), 1 µl plasmid (1 µg/ml), 5.5 µl ddH_2O. The compounds were gently mixed. The PCR program was 15 cycles of 96°C for 10 seconds and 60°C for 90 seconds. The DyeEx 2.0 Spin Kit (Qiagen) was used to remove dye terminators according to the manufacturer's protocol. 4 µl purified DNA and 16 µl Hi-Di formamide were incubated at 90°C for 3 minutes and final sequencing was performed in an ABI3130 genetic analyzer capillary sequencer (Applied Biosystems). The 3130 Data Collection Software v3.0 was employed for performing sequencing. The sequencing analysis software 5.2 (Applied Biosystems) was utilized for analyzing the results.

3.2.7 Enzyme Restriction

3 µl of plasmid (~700 ng) were added to 2 µl enzyme buffer 1, 2 µl 10×BSA, 2 µl AgeI, 2 µl EcoRV and ddH_2O to add up to 20 µl. The reagents were gently mixed and placed at 37°C in a water bath for 3 hours. The results were detected on a 1% agarose gel, and purified with the QIAquick Gel Extraction Kit (Qiagen).

3.3 Dual-reporter luciferase assays

The term "dual-reporter" refers to the simultaneous expression and measurement of two individual reporter enzymes. Typically, the experimental reporter contains the 3'-UTR of interest, while the control reporter provides an internal control. After transfection, cells are assayed by measuring the

experimental reporter activity normalized to the internal control (Xu et al., 2013).

Firstly, 3 x 10^4 H1299 cells were seeded per well of a 12-well plate. After 24 hours, cells were transfected with 100 ng empty pGL3 firefly reporter or the molar equivalent of a pGL3 construct. Additionally, 20 ng of Renilla reporter was co-transfected for normalization and either 25 nM of respective miRNA or nagative control oligonucleotide (Applied Biosystems) (Shi et al., 2014).

After 48 hours incubation, a Dual-Luciferase reporter assay (Promega) was performed according to the manufacturer's instructions. Luminescence intensities were measured with an Orion II illuminometer (Berthold) in 96-well format and analyzed with the SIMPLICITY software package (DLR) (Shi et al., 2014).

3.4 RNA isolation and Quantitative real-time PCR

3.4.1 Isolation of RNA and reverse transcription reaction

Total RNA extraction was performed using the High Pure RNA Isolation Kit (Roche) according to manufacturer's manual. Concentration and quality were tested with a Nanodrop spectrophotometer. Furthermore, 1 µg of total RNA was used for the reverse transcription reaction to generate cDNA with the verso cDNA Kit (Thermo Fisher Scientific).

For isolation of the small RNA fraction, especially microRNA enriched fraction, we employed the High Pure miRNA Isolation Kit (Roche) according to manufacturer's instructions.

3.4.2 Quantitative real-time PCR (qPCR)

In order to determine mRNA expression levels, the Fast SYBR Green Master Mix (Applied Biosystems) was applied for the real time PCR analysis. According to the standard protocol, 7.5 µl SYBR Green Master Mix, 5 µl H_2O, 1 µl cDNA and 1.5 µl Fwd-Rev mix primers (see 2.2.11) were added to each reaction. The program of the Light Cycler 480 System was as follows: 95°C for 20 seconds, 40 cycles of 95°C for 1 second, 60°C for 20 seconds and 72°C 1 for second, final 98°C for 10 seconds and 60°C for 1 minute. A house-keeping gene, namely *β-actin*, was required for the normalization of the results (Shi et al., 2014).

To detect mature miR-15a/16-1 expression, the miRCURY LNA™ Universal RT microRNA PCR Kit (Exiqon), and miR-15a/16-1 specific primers (Exiqon) combined with SYBR® Green master mix (Exiqon) were used in the Light Cycler 480 System. The gene of *SNORD48* served as the normalization of the results (Shi et al., 2014).

3.5 Protein extraction and Western blot analysis

3.5.1 Protein extraction

Pre-incubated cells were treated in the presence/absence of the respective compounds and reached the ideal confluence. The plate was transferred immediately on ice and washed twice with precooled 1×PBS. Protein was harvested using a scraper and RIPA buffer, which contained protease and phosphatase inhibitors (Roche). The cell lysate was transferred to a new tube and sonified using a HTU SONI130 device with the intensity of 85% amplitude 3 consecutive times and each time 5 seconds. Afterwards, the lysate was centrifuged at 13,000 rpm at 4°C for 20 minutes to separate supernatant and

debris. The protein lysate was transferred to a fresh tube for further protein concentration measurement or storage at -80°C immediately.

The BCA Protein Assay Kit (Pierce, Thermo Fisher Scientific) was utilized to measure protein concentration and the Skanlt RE Varioskan 2.4.3 algorithm (Thermo Fisher Scientific) was used to calculate the results.

3.5.2 Western blot analysis

Resolving gels were prepared with polyacrylamide concentrations of 10%, and covered with 4% stacking gels to analyze protein. 40-80 µg of protein was diluted with 2×Laemmli buffer with a final concentration of 5% β-mecaptoethanol (Sigma-Aldrich). The mixture was incubated at 95°C for 5 minutes to denature protein, and loaded on the gels between two pre-stained protein ladders (Fermentas). Then, electrophoresis was performed at 90 V for the stacking gel and 120 V for the resolving gel in a Mini-PROTEAN®-electrophoresis system (Bio-Rad) with 1×Tris-glycine-SDS running buffer.

In order to make the proteins accessible for antibody detection, proteins were transferred to an Immobilon-P polyvinylidene difluoride (PVDF) membrane (Millipore) using Towbin buffer. The PerfectBlue^{TM} SEDES 'Semi-Dry' blotting system (Peqlab) and the EPS 600 power supply (Pharmacia Biotech) at constant amperage of 100 mA per gel and a maximum voltage of 10 V for 30-90 minutes, depending on the size of the protein, were employed for Western blotting.

To prevent of non-specific interaction, the membrane was placed in 5% skim milk in TBST for one hour at room temperature. Subsequently, the membrane was incubated with primary antibodies (see 2.2.13) overnight at 4°C. The membrane was washed twice in 1×TBST for 15 minutes each time, followed by one hour incubation with the horseradish-peroxidase (HRP)-conjugated

respective secondary antibody (see 2.2.13). After that, the membrane was rinsed twice in TBST for 15 minutes each time and 2 minutes in TBS. Western Lightning™ Plus-ECL (Millipore Corporation) was used for abundantly expressed proteins (e.g. α-tubulin) and Immobilon™ Western (Millipore Corporation) for proteins with weak expression. The signals were visualized using a CF40 Imager (Kodak).

3.6 Boyden-chamber assay of migration and invasion

For the last 48 hours cells were deprived of serum (0.1%). To analyze migration, 5 x 10^4 cells were seeded in the upper chamber of the Boyden-chamber in serum free medium. To analyze invasion, membranes were coated with Matrigel (BD Bioscience) at a final concentration of 3.3 ng/ml in serum free medium. Then 7 x 10^4 cells were seeded on the Matrigel in the upper chamber. As chemo-attractant, medium with 10% FBS was placed in the lower chamber. Migration or invasion toward 0.1% serum was used as a control. Cultures were maintained for 48 hours. Afterwards, non-motile cells at the top of the chamber were removed with q-tips and the cells in the bottom chamber were fixed with methanol and stained with DAPI. Five different fields per condition were evaluated using immunofluorescence microscopy. The average number of cells in the five fields per membrane was calculated. Each condition was performed in triplicate. The relative migration/invasion was calculated by the ratio of treated cells to control cells. The p-value was computed with a t-test (Shi et al., 2014).

3.7 Immunofluorescence and confocal laser-scanning microscopy

For immunofluorescence analysis, cultivated cells on glass cover-slides were fixed in 4% paraformaldehyde for 10 minutes under the chemical hood and washed three times with phosphate buffered saline (PBS). The cells were then permeabilized in 0.2% Triton X 100/PBS for 20 minutes and blocked with 100% FBS for 1 hour. Primary and secondary antibodies are listed above (see 2.2.13). DNA was stained with DAPI (Roth). Specimens were covered with ProLong Gold antifade (Invitrogen). LSM (laser scanning microscopy) images were captured with a confocal microscope (LSM 700; Zeiss) using a Plan Apochromat 20x/0.8 M27 objective, the ZEN 2009 software (Zeiss) and the following settings: image size 2048x2048 and 16 bit; pixel/dwell of 25.2 µs; pixel size 0.31 µm; laser power 2%; master gain 600-1000. After image capturing the original LSM files were converted into TIFF files.

3.8 DNA content analysis by flow cytometry

Cells were washed with PBS and fixed by addition of ice-cold 70% ethanol, then incubated over night at -20°C. Cells were stained with staining solution. After incubation for one hour at 37°C, cells were analyzed by flow cytometry using a CFlow6 device (Accuri). The p-value was computed with a t-test.

3.9 Analysis of colon cancer samples

The colon cancer RNA sample collections and their analysis for AP4 protein expression were described previously (Jackstadt et al., 2013). miRNAs were isolated from 5 µm sections of FFPE tumor tissue samples after micro-dissection using the High Pure miRNA Isolation Kit (Roche) according to manufacturer's instructions. cDNA was synthesized using 100 ng of isolated RNA enriched for small RNAs as a template. qRT microRNA PCR was performed in the Light Cycler 480 System using primers specific of hsa-miR-15a. Data was normalized to *SNORD48* expression. All reactions were performed as technical duplicates. RT reactions and quantification were performed using the miRCURY LNA™ Universal RT microRNA PCR Kit (Exiqon) according to manufacturer's instructions (Shi et al., 2014).

3.10 Statistical analyses

All data are presented as the mean value ± S.D. if not indicated otherwise. Differences between individual groups were analyzed by paired *t* tests. *P* values of $p<0.05$=*, $p<0.02$=**, $p<0.001$=*** were considered as statistically significant. To determine the correlation coefficient (r) and the significance (p) between the expression of AP4 protein and miR-15a the Pearson's correlation algorithm was applied. Statistical analyses were performed using the SPSS software 19 package (SPSS Inc., Chicago, IL). The plots in Figure 20D and 24A were generated with the GraphPad Prism software 6 (GraphPad Software Inc., La Jolla, CA).

4 Results

4.1 p53 mediates down-regulation of AP4 after DNA damage

Previous results showed that AP4 is down-regulated after treatment with etoposide, which induces DNA damage (Jung et al., 2008). As DNA damage activates p53, we investigated whether AP4 repression is mediated by p53. We employed isogenic pairs of HCT116 and RKO CRC cell lines harboring either *p53+/+* or *p53-/-* genotypes generated by homologous recombination (Bunz et al., 1998; Sur et al., 2009). After induction of DNA damage by treatment with doxorubicin (DOXO), AP4 levels were decreased only in p53-proficient cell lines (Figure 5A and 5B). When the same cell lines were treated with Nutlin-3a, a specific inhibitor of the p53-E3-ligase MDM2 (mouse double minute 2 homolog), similar results were obtained (Figure 5C).

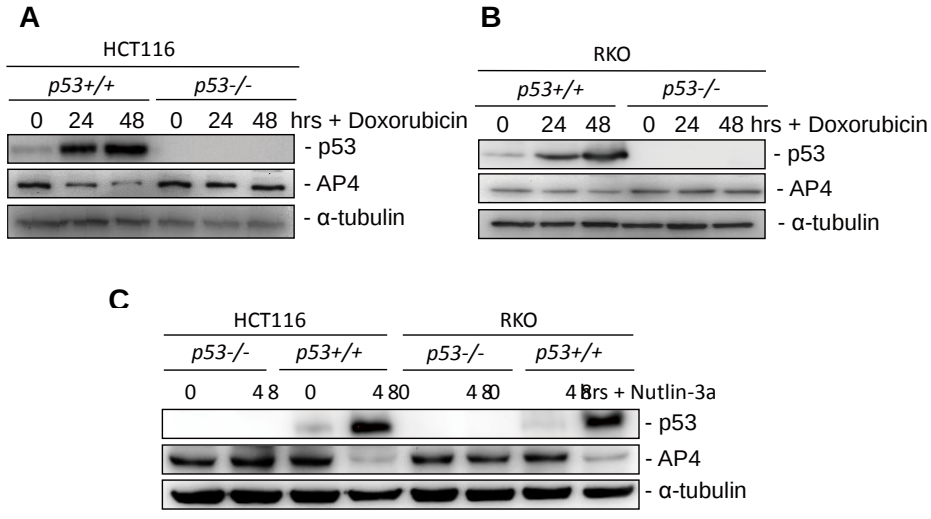

Figure 5 p53-dependent down-regulation of AP4 after DNA damage in HCT116 and RKO colorectal cancer cells

(A-C) Detection of the indicated proteins by Western blot analysis. α-tubulin served as a loading control. (A) HCT116 and (B) RKO cells with the indicated genotypes were treated with Doxorubicin (0.5 µg/ml) for the indicated periods. (C) HCT116 and RKO cells with the indicated genotypes were treated with Nutlin-3a (10 µM) for the indicated periods.

Furthermore, SW480/pRTR-p53-VSV pools were generated and treated with doxycycline (DOX). When p53 expression was induced, down-regulation of AP4 expression on the protein and mRNA levels was detected (Figure 6A and 6B).

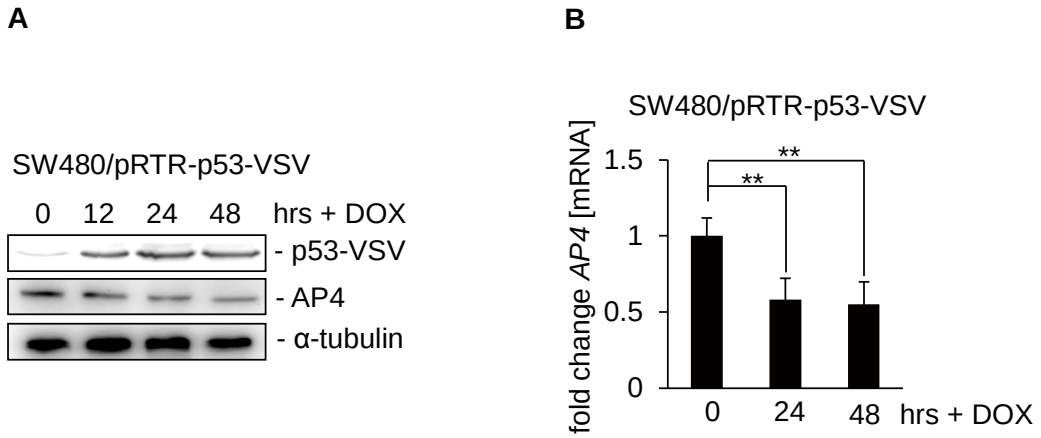

Figure 6 Down-regulation of AP4 by ectopic expression of p53

(A) Western blot analysis of the indicated proteins in SW480/pRTR-p53-VSV pools after treatment with DOX (100ng/ml) for the indicated periods. α-tubulin served as a loading control. (B) qPCR analysis of *AP4* mRNA expression in SW480/pRTR-p53-VSV pools after treatment of DOX for the indicated periods. B: results represent the mean value +/- S.D. (n=3).

Taken together, activation of p53 is necessary and mediates the down-regulation of AP4 in colon cancer cell lines.

4.2 AP4 is a direct target of miR-15a and miR-16-1

Our previous genome-wide ChIP-Seq analysis in the SW480 cell line ectopically expressing p53 did not show p53 occupancy within a distance of 30 kbp up- or down-stream of the *AP4* promoter (Hermeking et al., in preparation). Based on these results, *AP4* is presumably not a direct transcriptional target of

p53 indicating that there is probably another mediator involved in this regulation. Recently, several studies demonstrateded that miRNAs target the 3'-UTR of transcriptional factors and that these miRNAs also are induced by p53 (Kim et al., 2011b; Sachdeva et al., 2009; Siemens et al., 2011). Therefore, a reasonable explanation for the indirect down-regulation of AP4 by p53 could be that miRNAs participate in this pathway. Therefore, we conducted an *in silico* analysis with the *AP4* 3'-UTR using four different algorithms to identify putative miRNAs seed-matching sequences (Figure 7A). In each of the four algorithms, miR-15a, miR-101 and miR-144 were predicted to target the *AP4* 3'-UTR, whereas three algorithms identified potential target sites of miR-16-1 (Figure 7A). Interestingly, miR-15a and miR-16-1 are encoded by the same intron of the *DLEU2* precursor-RNA and belong to the same microRNA family. Both of them are induced by ectopic p53 (Fabbri et al., 2011; Suzuki et al., 2009). Since miR-101 and miR-144 are presumably not regulated by p53, we focused on miR-15a and miR-16-1 as putative mediators of AP4 down-regulation. Furthermore, the seed-matching sequences of miR-15a and miR-16-1 in the 3'-UTR of *AP4* are conserved among species, which may imply the functional importance of this sequence motif (Figure 7B).

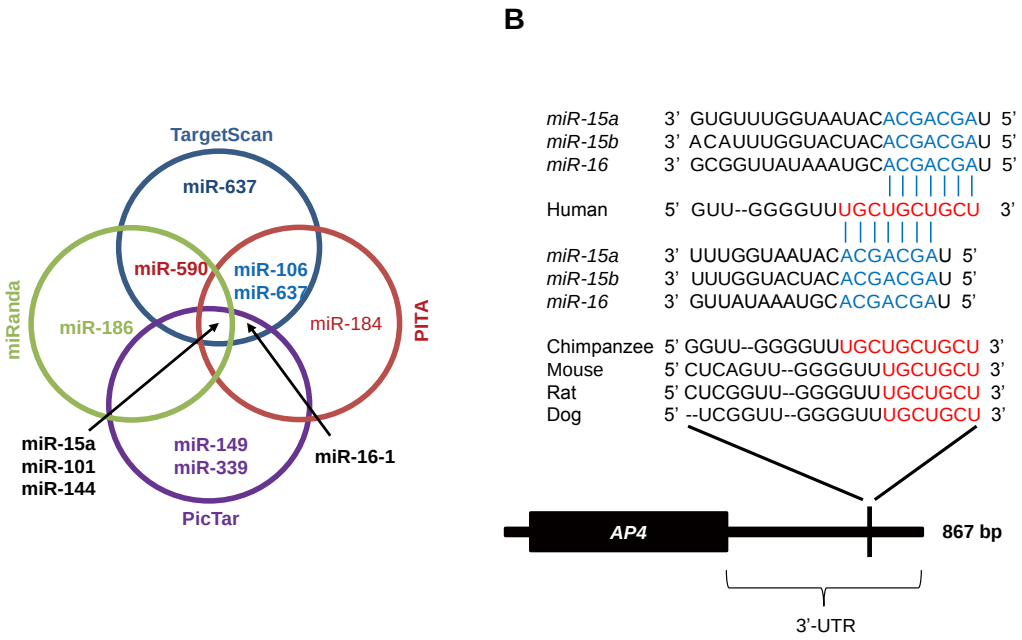

Figure 7 Bioinformatics identification of AP4 as a target of miR-15a/16-1

(A) Bioinformatics prediction of seed-matching sequences in the *AP4* 3'-UTR using four different algorithms. (B) Location and possible base-pairing within a predicted miR-15a/16-1 seed-matching sequences in the *AP4* 3'-UTR. Conservation of sequences is shown as red shading. Vertical lines represent probable base pairings.

After transfection of pre-miR-15a, pre-miR-16-1 or a combination of both pre-miRNAs into the colon cancer cell line SW480, AP4 was repressed dramatically (Figure 8A). Similar results were obtained after transfection of miR-15a/16-1 using the vector TW-miR-15a/16-1 in SW480 cells (Figure 8B). After transfection of *AP4*-specific siRNA, down-regulation of AP4 was detected in SW480 cells (Figure 8C). Transfection of pre-miR-15a, pre-miR-16-1 or a combination of both lead to a down-regulation of *AP4* on the mRNA level (Figure 8D). Notably, the combination resulted in a more pronounced repression of *AP4* than the single the pre-miRNAs, which suggests that miR-15a and miR-16-1 may cooperate on the two overlapping seed-matching sequences in the *AP4* 3'-UTR.

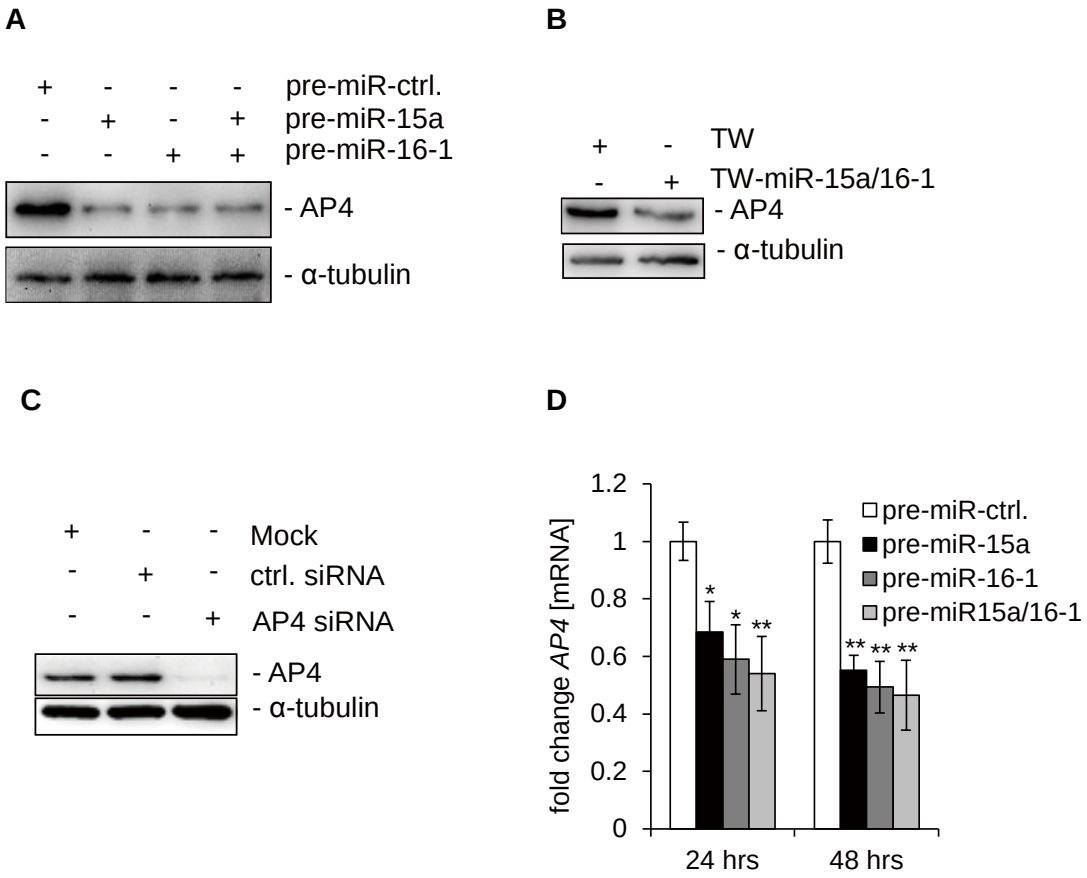

Figure 8 Repression of AP4 by miR-15a/16-1 in SW480 cells

(A) Western blot analysis of AP4 protein expression in SW480 cells after the transfection of the indicated pre-miR oligonucleotides (total 25 nM) for 48 hours. α-tubulin served as a loading control. (B) The indicated TW vector (4 µg/well) was transiently transfected into SW480 cells. The indicated proteins were detected. α-tubulin served as a loading control. (C) AP4-specific siRNAs transfected into SW480 cells resulted in decreased AP4 expression. (D) qPCR analysis of *AP4* mRNA after the transfection of pre-miR-15a and/or pre-miR-16-1 mimics (total 25 nM), for the indicated periods. D: results represent the mean value +/- S.D. (n=3). Rene Jackstadt performed the analyses and generated Figure 8 A and D.

H1299 cells were transfected with pre-miR-15a and pre-miR-16-1 oligonucleotides simultaneously with pGL3-AP4 3'-UTR and a construct encoding Renilla-luciferase. The two miRNAs lead to a similar and significant reduction of luciferase activity in dual-luciferase reporter system (Figure 9A). Furthermore, a reporter with mutated sequences in the seed-matching sites was resistant to down-regulation by pre-miR-15a and pre-miR-16-1 (Fig. 9B).

A

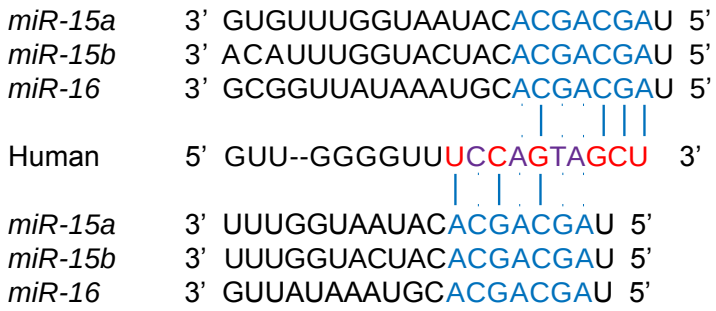

B

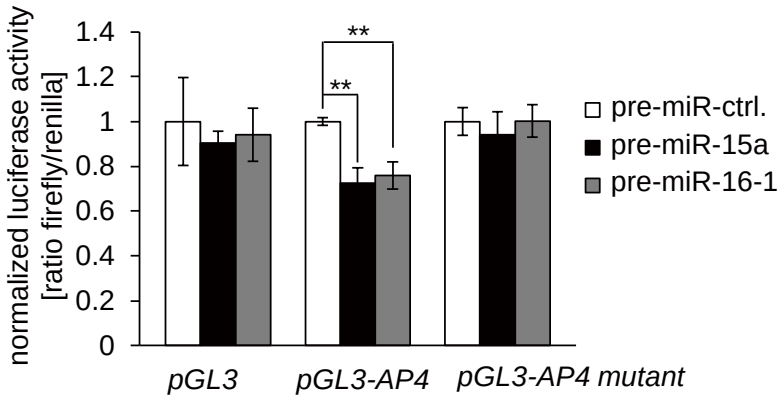

Figure 9 Regulation of AP4 by miR-15a/16-1 via a conserved seed-matching site

(A) *In vitro* mutagenesis of the miR-15a/16-1 seed-matching in the *AP4* 3'-UTR. Red shading indicates the conserved seed-sequences and blue letters indicate the mutations that had been included into the respective reporter constructs used in (B). (B) Dual-luciferase reporter analysis of the *AP4* 3'-UTR in H1299 cells 48 hours after transfection of pre-miR-15a or pre-miR-16-1. B: results represent the mean value +/- S.D. (n=3).

Collectively, the results indicate that miR-15a and miR-16-1 directly target the *AP4* 3'-UTR and repress AP4 expression by binding to these seed-matching sequences.

4.3 p53 decreases AP4 by p53 via miR-15a/16-1

In Figure 5A we showed that AP4 was repressed by p53 after DNA damage. Furthermore, DNA damage also resulted in a significant p53-dependent increase in mature miR-15a level (Figure 10A). After ectopic expression of p53 in SW480 cells, the induction of *pri-miR-15a/16-1* and repression of *AP4* mRNA were also observed (Figure 10B and 6B).

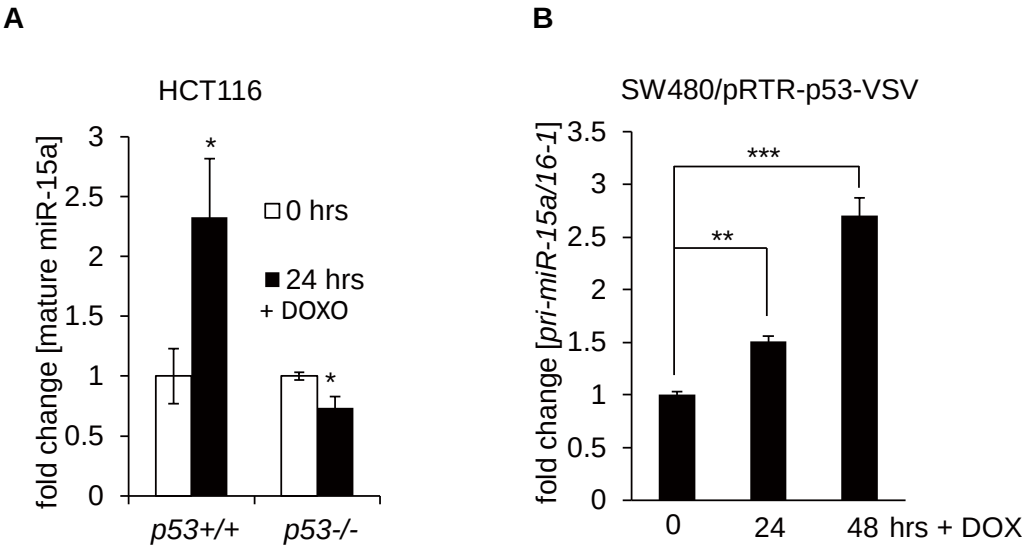

Figure 10 Up-regulation of miR-15a/16-1 by p53 in colon cancer cell lines

(A) HCT116 cells with the indicated genotype were treated with DOXO (0.5 µg/ml) for 24 hours. Then mature miRNAs were analyzed by qPCR. (B) qPCR analysis of *pri-miR-15a/16-1* expression after activation of p53 by addition of DOX for the indicated periods in SW480/pRTR-p53-VSV cells. A and B: results represent the mean value +/- S.D. (n=3).

In order to determine whether miR-15a/16-1 is required for the repression of AP4 by p53, we employed a miR-15a/16-1-specific sponge, which was previously described in (Bonci et al., 2008). Indeed, transfection of a plasmid encoding the miR-15a/16-1-specific sponge prevented the repression of AP4 after treatment with Nutlin-3a in HCT116 cells (Figure 11A). In p53-deficient HCT116 cells, AP4 expression was not affected by this reagent. Furthermore,

the induction of *pri-miR-15a/16-1* and repression of *AP4* mRNA could be prevented by transfection of the miR-15a/16-1-specific sponge into SW480 cells expressing a conditional *p53* allele (Figure 11B). Interestingly, treatment with the miR-15a/16-1-specific sponge could reverse the p53-induced down- or up-regulation of several genes involved in EMT and MET as *Snail*, *VIM* and *CDH1* on the mRNA level (Figure 11B). Furthermore, when the induction of miR-15a/16-1 was prevented by transfection of the miR-15a/16-1-specific sponge, the repression of migration by ectopic 53 was alleviated in SW480/pRTR-p53-VSV cells (Figure 11C).

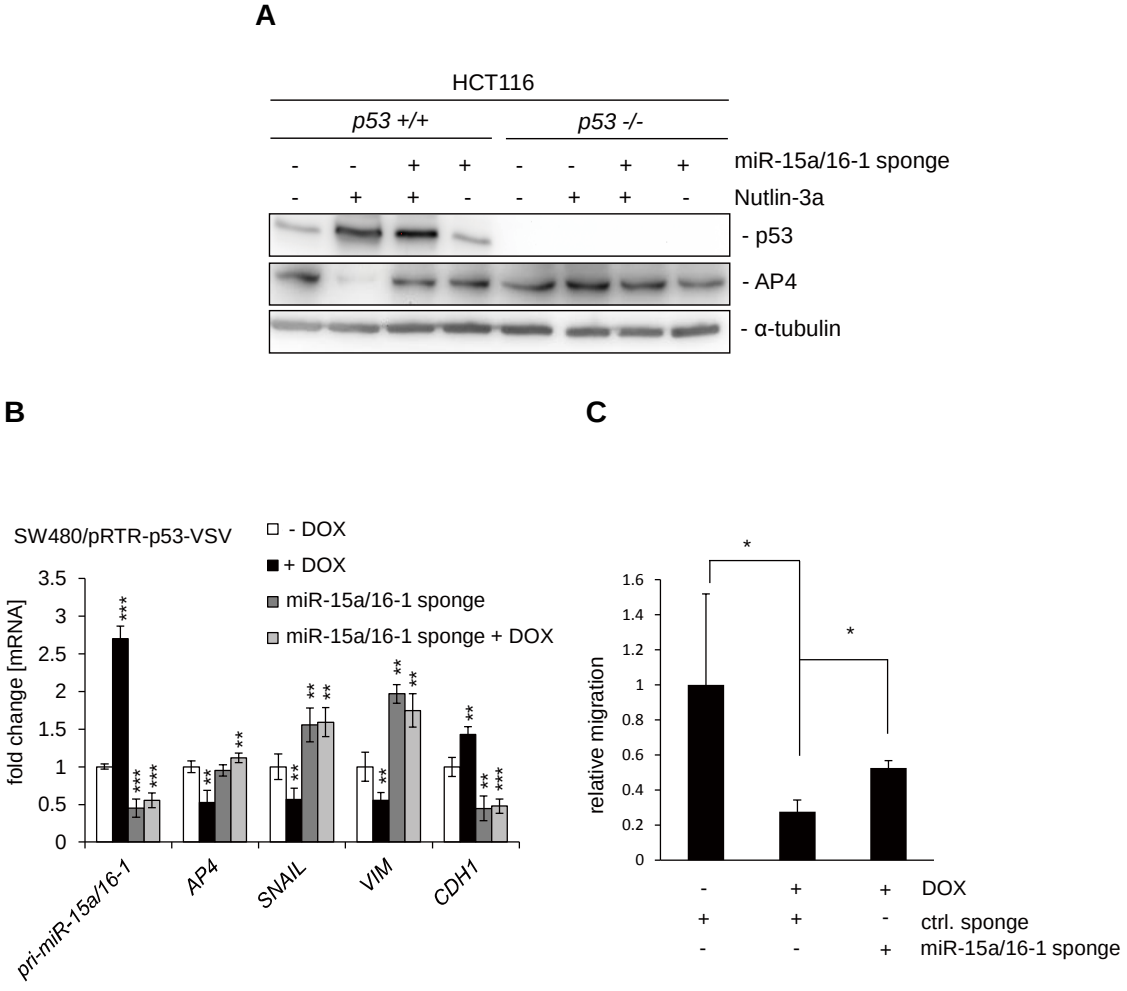

Figure 11 p53 represses AP4 and EMT- related markers via miR-15a/16-1

(A) HCT116 cells with the indicated genotype were transfected with plasmids encoding the miR-15a/16-1-specific sponge for 24 hours and subsequently treated with Nutlin-3a for 48 hours. The indicated proteins were detected by Western blot analysis. α-tubulin served as a loading control. (B) SW480/pRTR-p53-VSV cells were

transfected with the miR-15a/16-1-specifc sponge for 24 hours and subsequently DOX was added for 48 hours. The indicated mRNAs were detected by qPCR. (C) Determination of migration in a transwell Boyden-chamber assay in SW480/pRTR-p53-VSV cells. First, cells were transfected with the miR-15a/16-1-specific sponge or control sponge for 24 hours and subsequently DOX was added for 48 hours. For the last 48 hours, the serum concentration was reduced to 0.1%. In the end, cells were fixed and stained with DAPI. The average numbers of cells in five fields per membrane were recorded in three different inserts. Relative migration is given in the value of test cells to control cells. B and C: results represent the mean value +/- S.D. (n=3).

In summary, these data reveal that the repression of AP4 by p53 is mediated by miR-15a/16-1 and that p53 inhibits EMT in SW480 cells via inducing miR-15a/16-1.

4.4 miR-15a/16-1 induces MET by repressing AP4

Recently, our group revealed that AP4 induces EMT, promotes migration/invasion and contributes to metastasis by directly regulating SNAIL and E-cadherin expression (Jackstadt et al., 2013). This data suggest that ectopic expression of miR-15a and miR-16-1 could induce MET and repress metastasis by repressing AP4 expression. Indeed, transfection of pre-miR-15a and pre-miR-16-1 in the mesenchymal cell line SW480 negatively regulated EMT-related markers and further induced MET. The mesenchymal markers *SNAIL* and *VIM* were significantly repressed while the epithelial marker *CDH1* was up-regulated on the mRNA level (Figure 12).

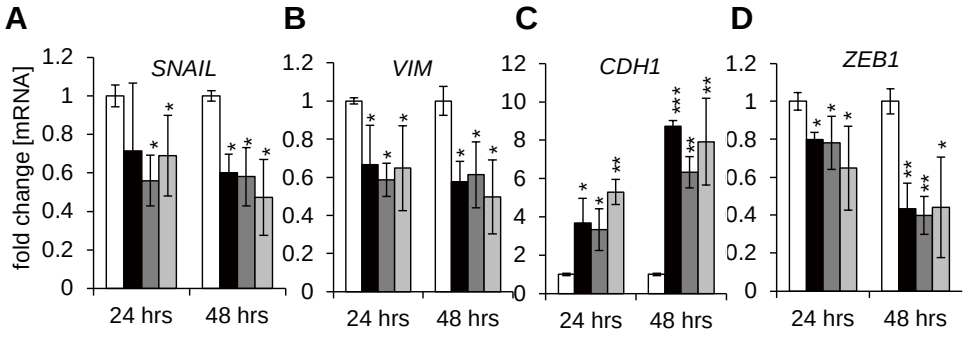

Figure 12 Regulation of EMT-related markers by transfection of pre-miR-15a and pre-miR-16-1 in SW480 cells

Expression of the indicated mRNAs (A) *SNAIL* (B) *VIM* (C) *CDH1* (D) *ZEB1* was determined by qPCR analysis after transfection of the indicated pre-miRNAs (total 25 nM) for the indicated periods. Results represent the mean value +/- S.D. (n=3). Rene Jackstadt performed the analyses and generated the figures.

Similar results were obtained using the *pri-miR-15a/16-1* conditional overexpression system in SW480 cells (Figure 13A, 13B and 13C). The epithelial marker E-cadherin was up-regulated on both protein and mRNA levels after ectopic miR-15a/16-1 expression (Figure 13A and 13B), whereas the mesenchymal markers *SNAIL* and *VIM* were repressed on the mRNA level (Figure 13C). An immunofluorescence analysis confirmed the down-regulation of AP4 and SNAIL after ectopic expression of miR-15a/16-1 (Figure 13D).

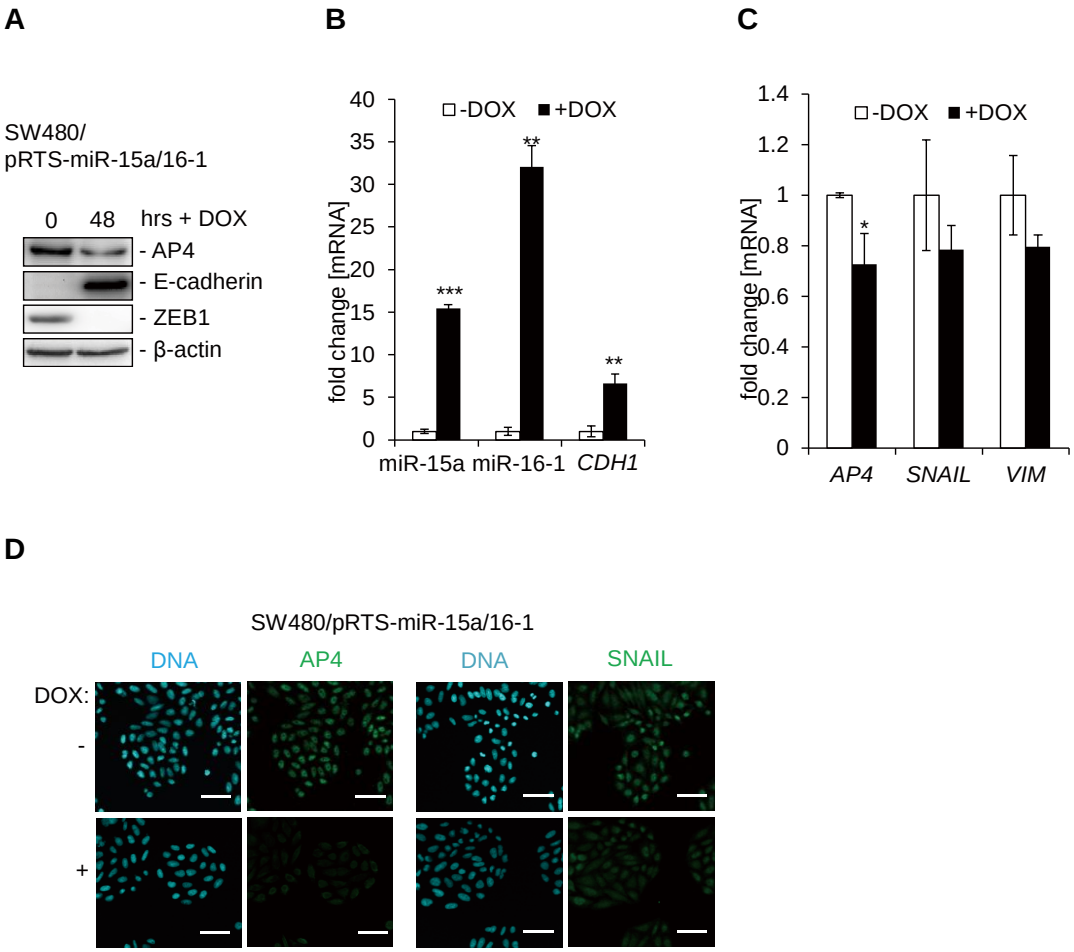

Figure 13 Regulation of EMT-related markers by ectopic expression of miR-15a/16-1

(A) Western blot and (B and C) qPCR analysis of the indicated protein, miRNAs and mRNAs after 48 hours addition of DOX in SW480/pRTS-miR-15a/16-1 cells. (D) 72 hours after the addition of DOX, SW480/pRTS-miR-15a/16-1 cells were stained and subjected to confocal microscopy. Nuclear DNA was detected by DAPI staining. Scale bars represent 50 µm. B and C: results represent the mean value +/- S.D. (n=3).

In addition, overexpression of miR-15a/16-1 inhibited wound closure in SW480/pRTS-miR-15a/16-1 cells (Figure 14A and 14B). A significant repression of migration and invasion was also detected in a Boyden-chamber assay (Figure 14C).

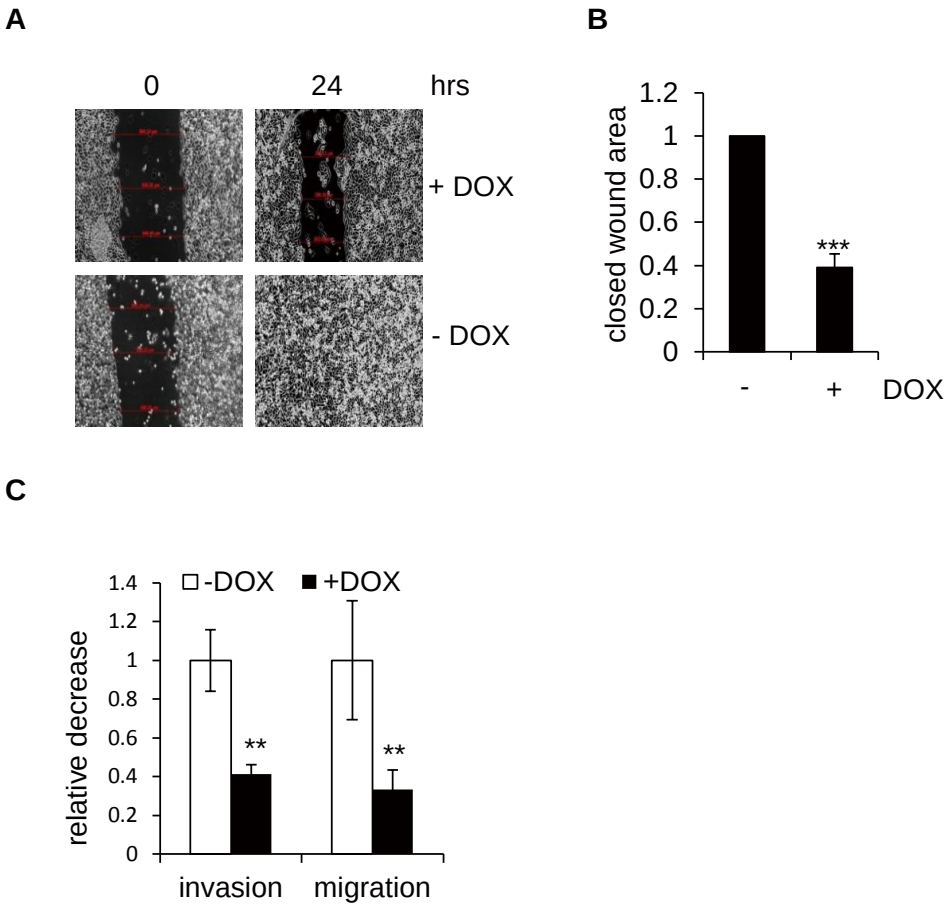

Figure 14 Ectopic miR-15a/16-1 inhibits would closure, invasion and migration

(A) Representative pictures and (B) quantification of a wound healing assay after 72 hours activation of miR-15a/16-1 in SW480/pRTS-miR-15a/16-1 cells. Wound closure was determined 48 hours after scratching. Mitomycin C was applied for 2 hours before scratching. (C) Determination of invasion and migration of SW480/pRTS-miR-15a/16-1 cells as described in Figure 11C. To analyze invasion, membranes were coated with Matrigel (3.3 ng/ml in the respective medium). A, B and C: results represent the mean value +/- S.D. (n=3).

Then, the TargetScan algorithm was used to analyse the 3'-UTRs of other known EMT-related factors, e.g. SNAIL1, SNAIL2, CDH1, ZEB1, ZEB2 and TWIST1. As shown in Figure 15, a putative miR-15a/16-1 seed-matching site could not be detected in the 3'-UTR of other EMT-inducing TFs. Therefore, AP4 presumably represent the only known EMT-TF, which is directly targeted by miR-15a/16-1.

A

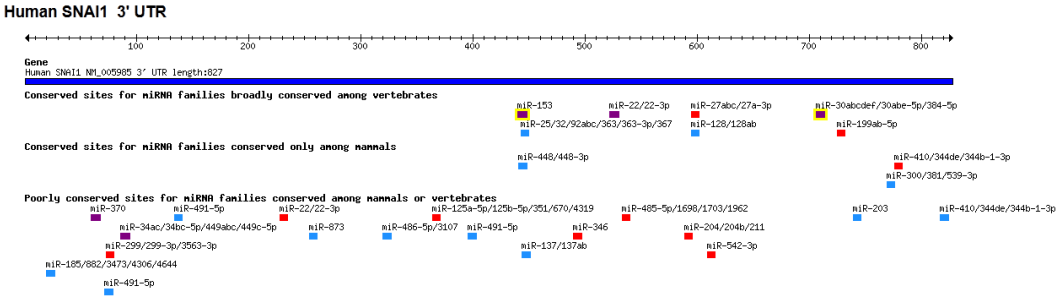
Human SNAI1 3' UTR
Gene
Human SNAI1 NM_005985 3' UTR length:827
Conserved sites for miRNA families broadly conserved among vertebrates
Conserved sites for miRNA families conserved only among mammals
Poorly conserved sites for miRNA families conserved among mammals or vertebrates

B

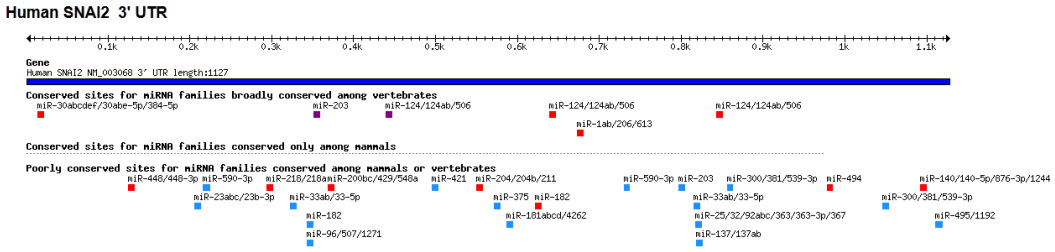
Human SNAI2 3' UTR
Gene
Human SNAI2 NM_003068 3' UTR length:1127
Conserved sites for miRNA families broadly conserved among vertebrates
Conserved sites for miRNA families conserved only among mammals
Poorly conserved sites for miRNA families conserved among mammals or vertebrates

C

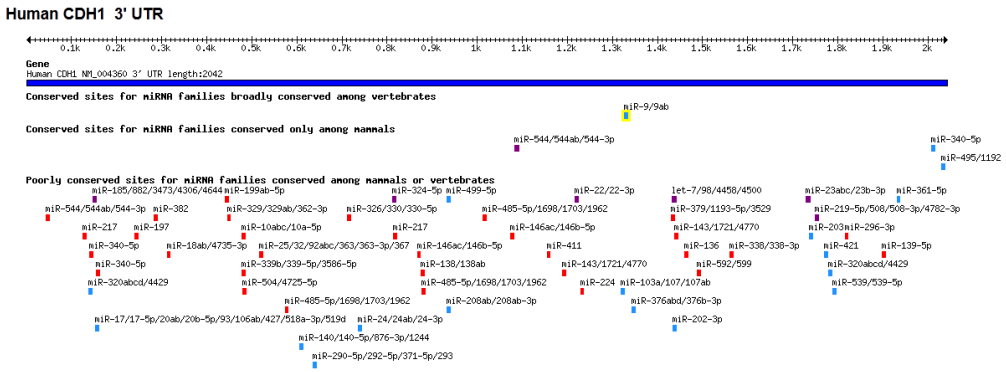
Human CDH1 3' UTR
Gene
Human CDH1 NM_004360 3' UTR length:2042
Conserved sites for miRNA families broadly conserved among vertebrates
Conserved sites for miRNA families conserved only among mammals
Poorly conserved sites for miRNA families conserved among mammals or vertebrates

D

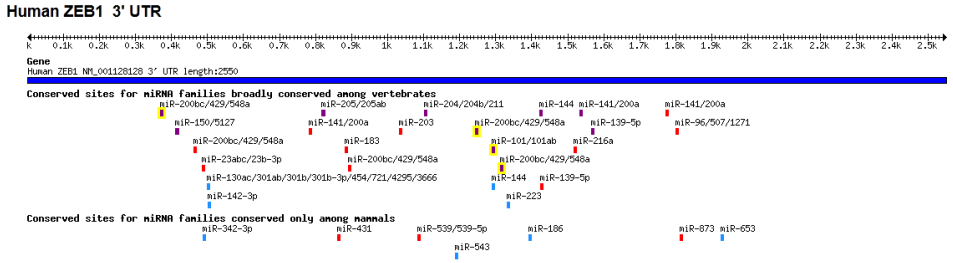
Human ZEB1 3' UTR
Gene
Human ZEB1 NM_001128128 3' UTR length:2550
Conserved sites for miRNA families broadly conserved among vertebrates
Conserved sites for miRNA families conserved only among mammals

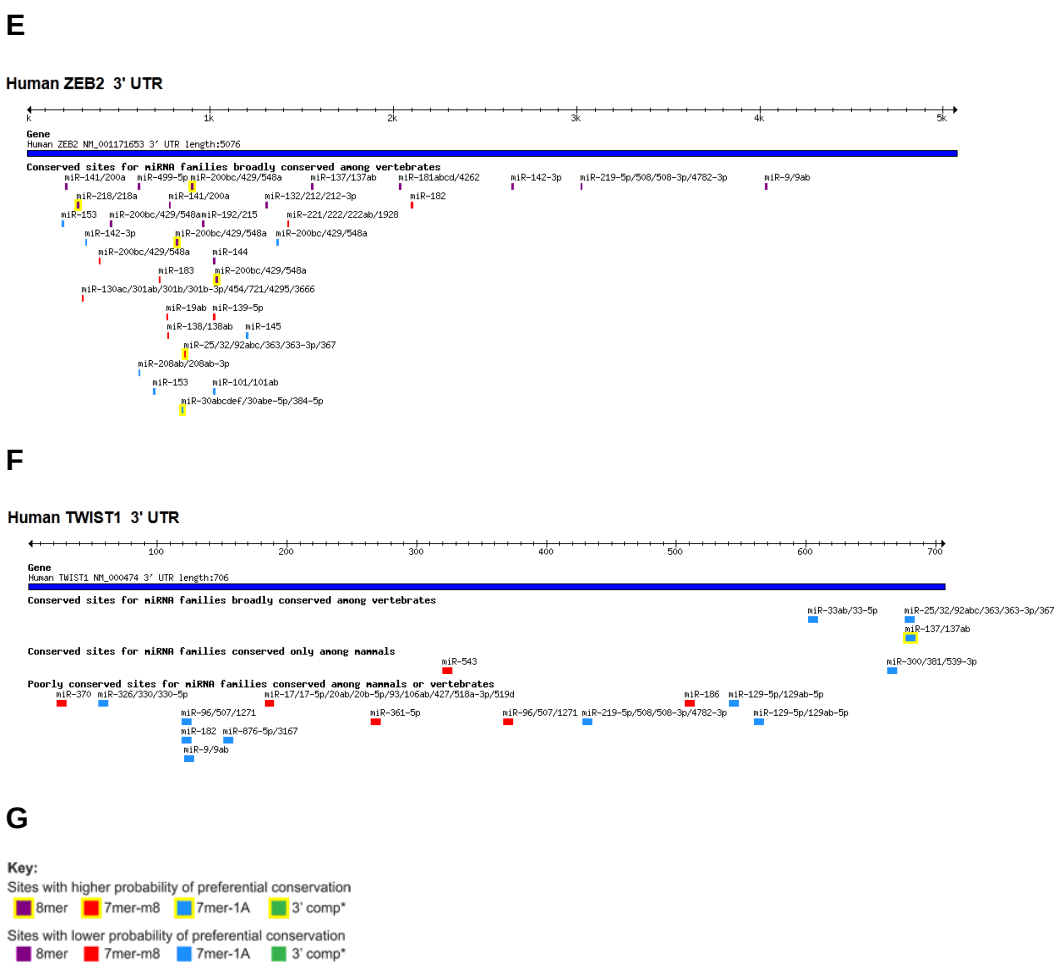

Figure 15 Bioinformatics prediction of seed-matching sequences in the 3'-UTR of other EMT-inducing transcription factors

In silico analysis of the 3′-UTR of EMT- inducing transcription factors. The 3′-UTRs of (A) SNAI1, (B) SNAI2, (C) CDH1, (D) ZEB1, (E) ZEB2, and (F) TWIST1 were analyzed for the presence of miRNAs seed-matching sequences by using the algorithm of TargetScan. (G) Color keys indicated the degree of seed/seed-matching sequence conservation.

In support of this notion, the repression of migration by overexpression of miR-15a was alleviated after ectopic expression of AP4 in a conditional expression system, which lacks its original 3'-UTR (Figure 16).

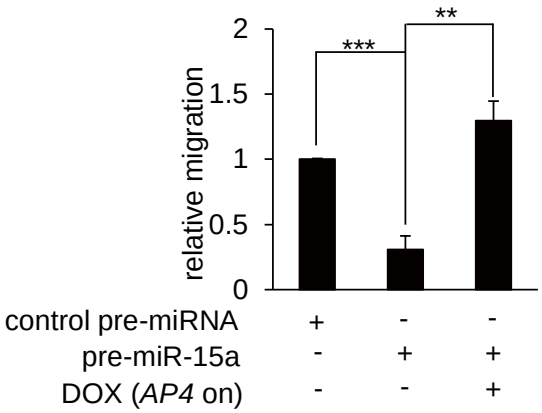

Figure 16 Inhibition of migration by miR-15a/16-1 is attenuated by ectopic AP4 expression

After 72 hours treatment with DOX or vehicle, SW480/pRTR-AP4-VSV cells were transfected with the indicated oligonucleotides; 24 hours before seeding the cells on the Boyden-chamber membrane, serum was reduced to 0.1% as described in Figure 11C. Results represent the mean value +/- S.D. (n=3).

Collectively, these results demonstrate that miR-15a/16-1 inhibits EMT by repressing AP4 in SW480 cells.

4.5 Role of AP4 in cell cycle inhibition by *miR-15a/16-1*

Recently, several reports showed that miR-15a/16-1 induces apoptosis and inhibits cell cycle progression by targeting BCL2 and CCND1, respectively (Bonci et al., 2008; Chen et al., 2008; Cimmino et al., 2005). In contrast to that, AP4 promotes cell proliferation, at least in part, by repressing the cyclin-dependent kinase (CDK) inhibitor p21 (Jung et al., 2008). Here, we hypothesized that the miR-15a/16-1/AP4 axis inhibits cell cycle progression in colorectal cancer cells. After transfection of pre-miR-15a, it caused a pronounced and significant G_1 arrest in SW480 CRC cells (Figure 17A and 17B). When a conditional *AP4* allele lacking its 3'-UTR, therefore being resistant to miR-15a/16-1, was activated simultaneously with the transfection

of miR-15a, a G_1 arrest was prevented and cells continued to cycle, as indicated by an unchanged amount of cells in the G_1 and S phase.

Consequently, down-regulation of AP4 by miR-15a/16-1 is not only necessary for mediating EMT, but also plays a key role in the inhibition of the cell cycle progression by miR-15a/16-1 in colon cancer cells.

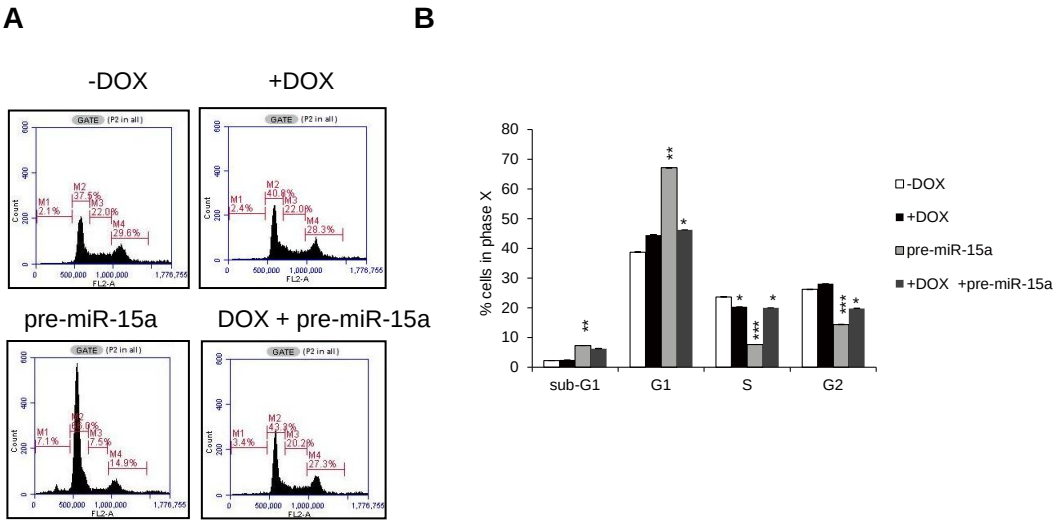

Figure 17 G_1 arrest by miR-15a/16-1 is rescued by ectopic AP4 expression

(A and B) Cell cycle distribution as determined by DNA content analysis using flow cytometry. SW480/pRTR-AP4-VSV cells were treated with DOX or vehicle for 72 hours, and the last 24 hours transfected with the indicated oligonucleotides, then cells were fixed and DNA was stained with propidium iodide. Results represent the mean value +/- S.D. (n=3).

4.6 miR-15a/16-1 represses metastasis of CRC Xenografts

Tsai *et al* demonstrated that activation of EMT promotes local tumor invasion, intravasation and extravasation of systemic circulation (Tsai et al., 2012). Therefore, we further investigated the role of miR-15a/16-1 in the lung metastases formation using engrafted SW620 cells in mice. Hence, we stably introduced a *luciferase 2 (luc2)* and *miR-15a/16-1* expression cassette using

lentiviral transduction in SW620 colorectal cancer cells. Furthermore, overexpression of *miR-15a/16-1* decreased AP4 expression on the protein and mRNA levels (Figure 18A and 18B). Moreover, mesenchymal markers like *SNAIL* and *VIM* were down-regulated (Figure 18B). Additionally, migration and invasion were repressed by ectopic miR-15a/16-1 expression as determined in a transwell Boyden-chamber assay (Figure 18C).

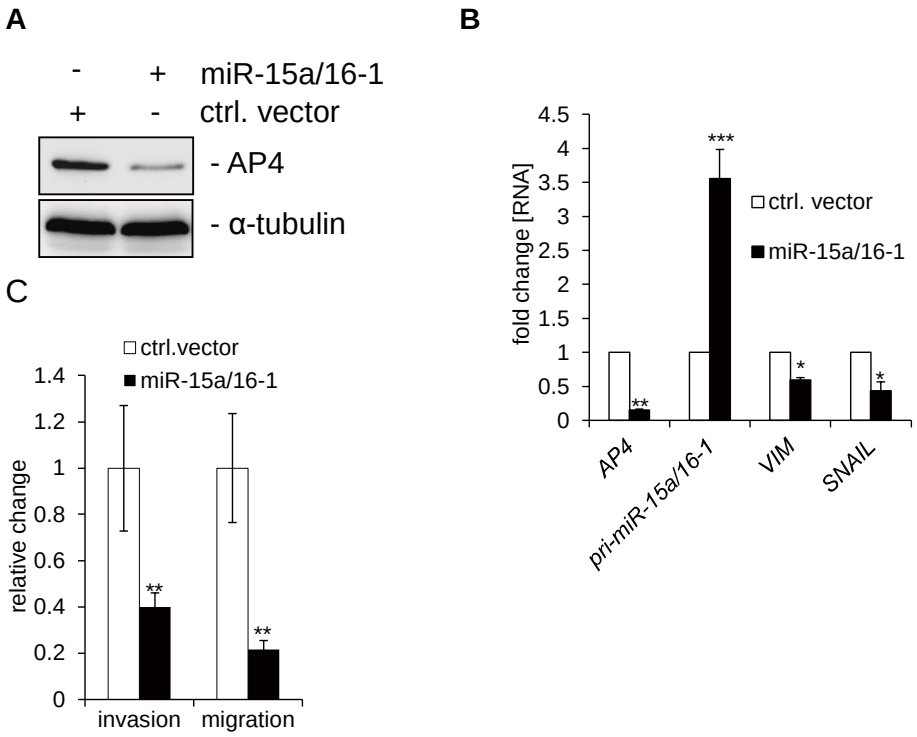

Figure 18 Stable expression of miR-15a/16-1 inhibits AP4 expression, mesenchymal markers, migration and invasion

(A) Western blot analysis of AP4 protein expression and (B) qPCR analysis of the indicated RNAs in SW620-Luc2 cells stably expressing miR-15a/16-1 or the respective control vector. α-tubulin served as a loading control. (C) Transwell Boyden-chamber assay of cellular migration and invasion of SW620-Luc2 cells. After 72 hours, cells were seeded into a transwell chamber and analyzed as described in Figure 11C. B and C (left panel): results represent the mean +/- S.D. (n=3). C (right panel): results represent the mean value +/- S.D. (n=2). Rene Jackstadt performed the analyses and generated the Figures 18A and B.

However, overexpression of miR-15a/16-1 did not cause a reduced proliferation in SW620 cells (Figure 19). This may be due to the lower levels of miR-15a/16-1 driven by the lentiviral vector compared to those resulting from transient transfection of pre-miR-15a in the experiments shown in Figure 17.

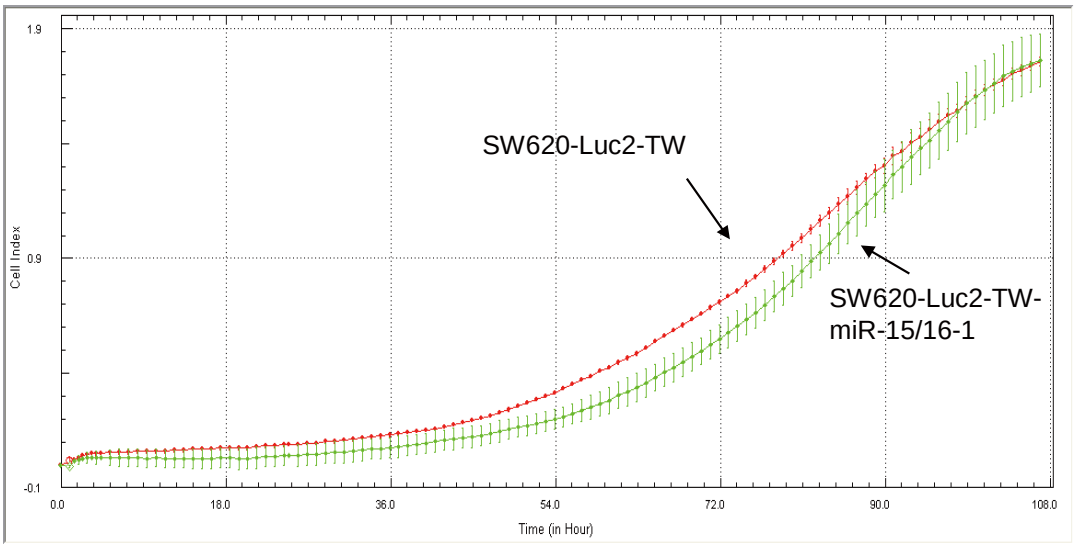

Figure 19 Analysis of cell proliferation in SW620-Luc2 cells harboring a miR-15a/16-1 vector or empty vector

Stable expression of miR-15a/16-1 did not lead to a decreased proliferation in SW620-Luc2 cells. Rene Jackstadt performed the analyses and generated the figure.

The cells harboring the miR-15a/16-1 stable expression or a control vector were injected in the tail vein of immune-compromised non-obese diabetic/severe combined immune-deficient (NOD/SCID) mice. Then, the spreading and colonization of cells was monitored over time in a non-invasive manner using luminescence imaging. Within four weeks, lung metastases were detected. In particular, weaker luminescence signals were detected in mice injected with miR-15a/16-1 expressing cells compared to control cells after nine weeks (Figure 20A and 20B). The number of lung metastases in the control group was higher than in the group treated with miR-15a/16-1 expressing cells (Figure 20C, left panel). Hematoxylin and eosin (H&E)

staining showed ectopic expression of miR-15a/16-1 repressed colonization of SW620 cells in the lung (Figure 20C, right panel). Furthermore, the total number of metastatic nodules declined as a result of ectopic expression of miR-15a/16-1 detected by histological quantification of the lung (Figure 20D). In summary, these results show that miR-15a/16-1 represses metastatic colonization and growth of CRC tumor cells *in vivo*.

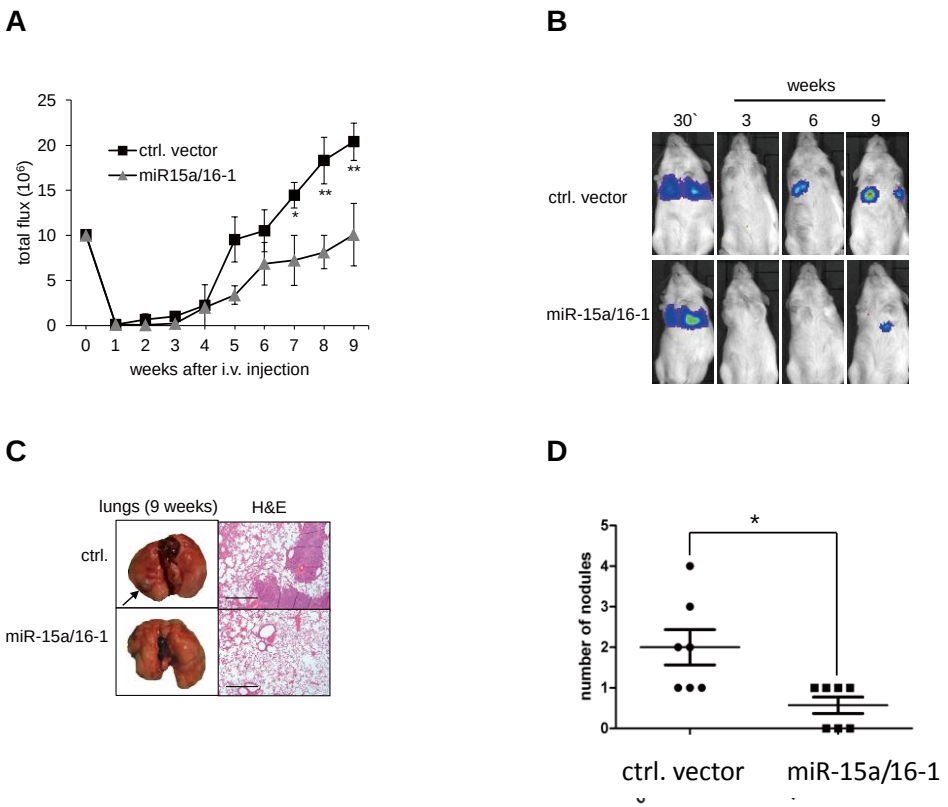

Figure 20. miR-15a/16-1 suppresses lung metastases formation *in vivo*

(A) SW620-Luc2 cells were introduced into NOD/SCID mice (n=7 for each group) by tail vein injection. Bioluminescence signals were recorded at the indicated time-points. Bioluminescence signals collected per mouse were depicted as “total flux”. (B) Representative bioluminescence images were recorded at the indicated time-points after injection. (C, left panel) Lungs were resected 9 weeks after injection. Arrows indicate metastatic tumor nodules. (C, right panel) Representative examples of the H&E staining of the resected lungs are shown. Scale bars represent 100 µm. (D) Quantification of metastatic tumor nodules in lung per mouse. Results represent the mean value +/- S.D. (n=7). Rene Jackstadt performed the analyses and generated the Figure 20A-D.

4.7 AP4 directly represses miR-15a/16-1

miRNAs often form feedback loops with transcriptional factors (Ebert and Sharp, 2012). Therefore, we hypothesized that AP4 may directly repress miR-15a/16-1 expression. In fact, the expression of primary and mature miR-15a/16-1 was decreased significantly after ectopic *AP4* expression in SW480/pRTR-AP4-VSV cells (Figure 21A and 21B). On the other hand, down-regulation of AP4 by two AP4-specific miRNAs caused an up-regulation of the *pri-miR-15a/16-1* transcript in SW480 (Figure 21C).

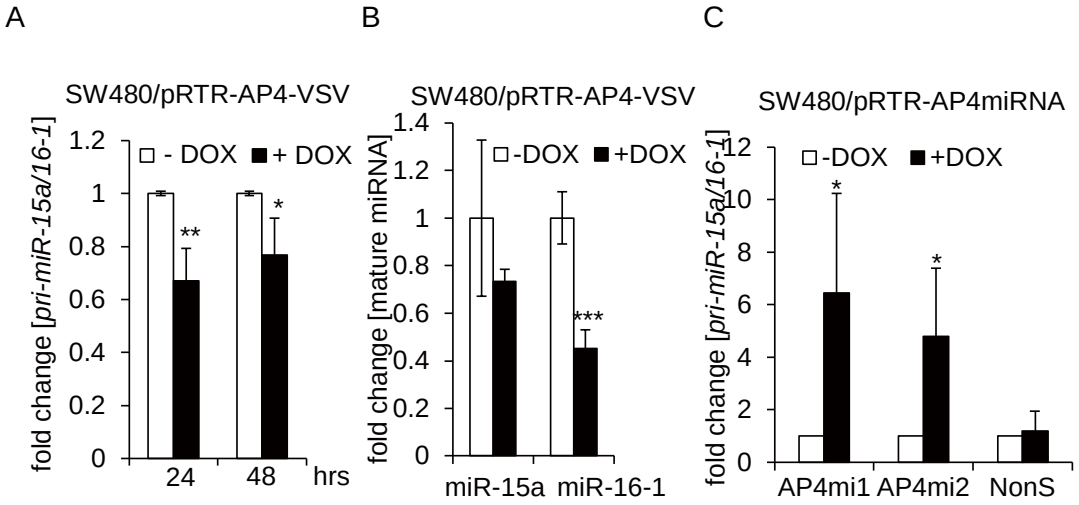

Figure 21. Activated AP4 represses miR-15a/16-1 expression in SW480 cell line

qPCR analysis of miR-15a/16-1 expression in SW480/pRTR-AP4-VSV cells after addition of DOX for the indicated periods (A) or 48 hours (B). (C) *pri-miR-15a/16-1* expression was detected in SW480 cells harboring episomal plasmids for conditional expression of two different miRNAs directed against AP4 (AP4mi1 or AP4mi2) or a non-silencing miRNA (NonS). Cells were treated with DOX for 48 hours. A, B and C: results represent the mean value +/- S.D. (n=3). Rene Jackstadt performed the analyses and generated Figure 21C.

Furthermore, ChIP followed by the next generation sequencing (ChIP-Seq) was employed in DLD-1/pRTR-AP4-VSV pools ectopically expressing AP4.

The data revealed that AP4 occupies regions in the vicinity of the two alternative *DLEU2* transcription start sites (Figure 22), the host gene of *miR-15a/16-1*.

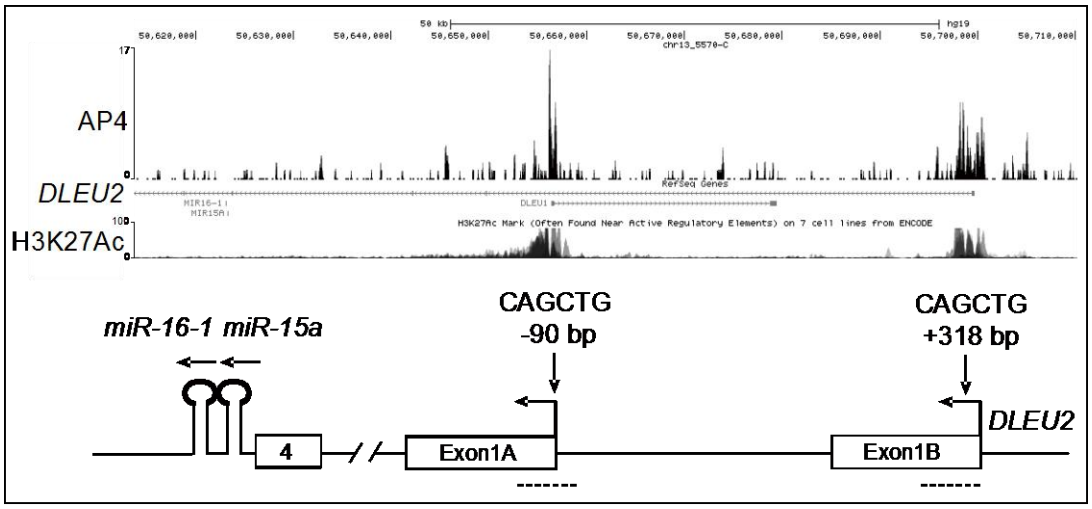

Figure 22. AP4 occupies the two *DLEU2* transcription start sites

(Upper panel) Representation of ChIP-Seq results obtained after ectopic expression of *AP4* for 24 hours in DLD-1 cells. Results were visualized by using the UCSC genome browser. (Lower panel) Schematic map of the human *DLEU2* locus. AP4 binding motifs are indicated by vertical arrows above the gene. Dashed lines indicate the amplicons used for qChIP analysis. Exons are indicated by rectangles and miRNAs by hairpins. Rene Jackstadt performed the analyses and generated the figure.

These results were further confirmed by qChIP in DLD-1 cells with activated AP4 expression (Figure 23A). Additionally, occupancy by endogenous AP4 was detected at *DLEU2* promoters in SW620 cells (Figure 23B).

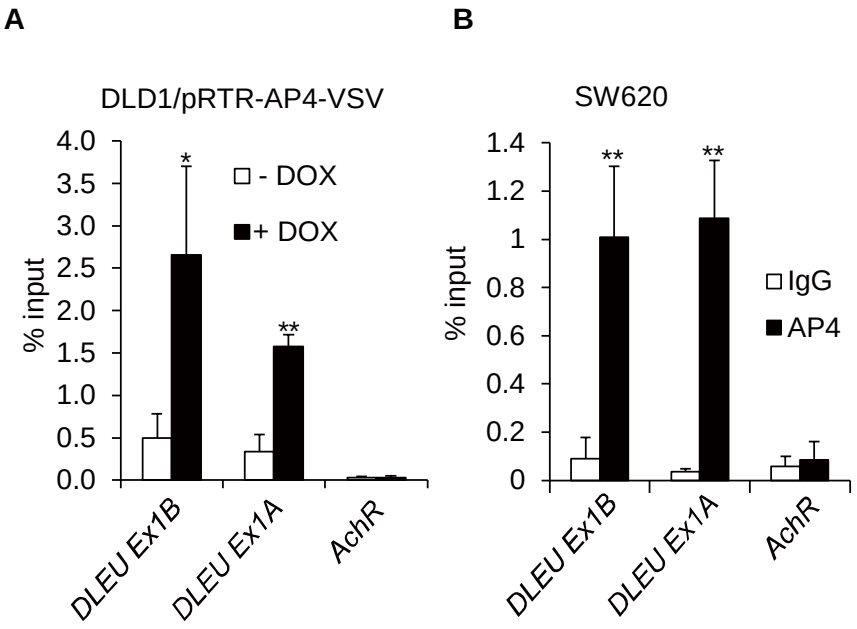

Figure 23 Regulation of miR-15a/16-1 by AP4

(A) DLD-1/pRTR-AP4-VSV cells were treated with DOX for 24 hours and subjected to qChIP analysis with an AP4-specific or, as a reference, IgG antibody. *AchR* amplification served as a control. (B) SW620 cells were subjected to qChIP analysis with an AP4-specific or, as a reference, IgG antibody. *AchR* amplification served as a control. A and B: results represent the mean value +/- S.D. (n=3). Rene Jackstadt performed the analyses and generated Figure 23 A and B.

Taken together, AP4 and miR-15a/16-1 generate a double-negative feedback loop and they can regulate each other.

4.8 Inverse correlation between AP4 and miR-15a/16-1 expression in primary CRC

As described above, we demonstrated that AP4 and miR-15a/16-1 form a double-negative feedback loop in colon cancer cell lines. Next, we determined whether they display a negative correlation in human patient samples. Therefore, we extracted small RNA fractions and detected the miR-15a expression from 94 colon cancer samples of a case-control cohort of matched

patients with and without distant liver metastasis. AP4 protein expression was detected as described in (Jackstadt et al., 2013). All data supported a significant negative correlation between AP4 and miR-15a. In fact, increased expression of AP4 inversely correlated with decreased miR-15a expression (Figure 24A). Particularly, only two of the ten cases with the most remarkable miR-15a expression showed an AP4 expression higher than the median, whereas eight samples with the lowest miR-15a expression presented AP4 expression above the overall average (Table II). In addition, five of the samples with lowest miR-15a expression were from patients that developed liver metastases within five years after resection of the primary tumor, while only two of those with the highest miR-15a expression showed distant metastases. Using the Oncomine database, we could observe a significant inverse correlation between *DLEU2* and *AP4* (Figure 24B) in the Notterman *et al* dataset (Notterman et al., 2001). AP4 expression was up-regulated in the cancer samples compared to normal cases, whereas *DLEU2* was repressed.

Table II Sub-analysis using cases with the most prominent miR-15a expression levels

	AP4 'high'	AP4 'low'
top 10 miR-15a	2	8
bottom 10 miR-15a	8	2

	Metastases (M1)	no Metastases (M0)
top 10 miR-15a	2	8
bottom 10 miR-15a	5	5

The top ten cases of high and low miR-15a expression were analyzed regarding their expression of AP4 and the presence/absence of liver metastases. AP4, high and low categorizations were based on the overall-median. p-values were calculated applying the Student's t-test. Helge Siemens performed the analyses and generated the Table II.

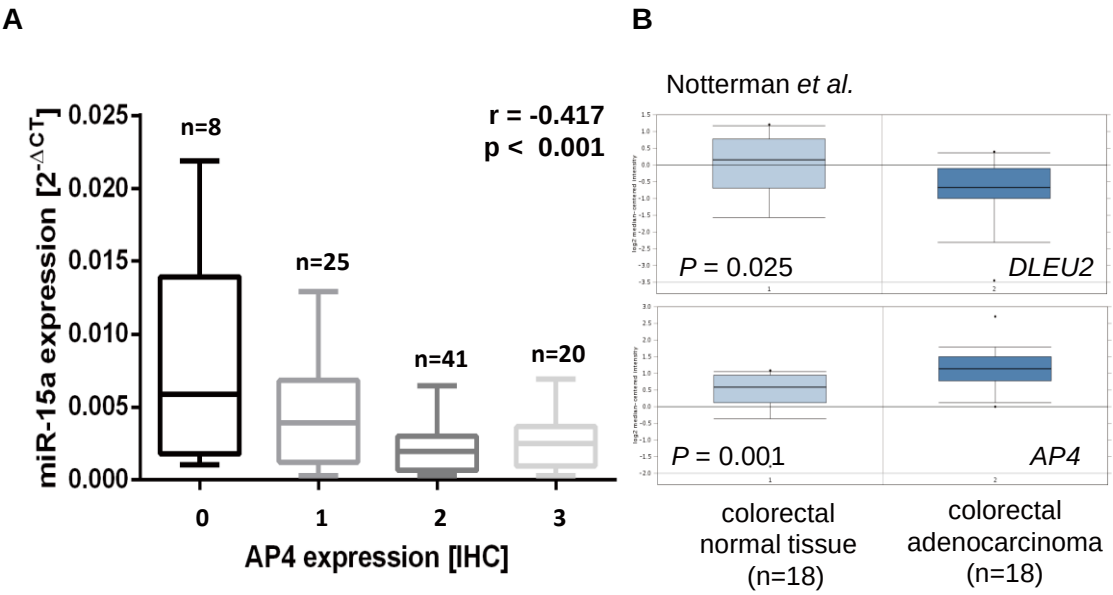

Figure 24 Inverse correlations of AP4 and miR-15a/16-1 expression in colon cancer samples

(A) 94 samples of right sided colon cancer were subjected to Exiqon qPCR analysis of miR-15a expression. AP4 protein expression was previously determined by using immunohistochemistry and was linked to miR-15a expression. The AP4 expression levels were assigned to four groups representing none (0), weak (1), moderate (2) and strong (3) expression. Significance and correlation coefficient were calculated with the Pearson correlation algorithm. (B) Analysis of mRNA expression levels of the indicated genes as deposited in the Oncomine database. Light blue indicates samples from normal colorectal tissue. Dark blue indicates samples from colorectal adenocarcinomas. P-values were provided by the Oncomine database. Helge Siemens performed the analyses and generated Figure A.

Collectively, an inverse correlation of miR-15a/16-1 and AP4 expression is also detectable in human colon cancer samples.

5 Discussion

5.1 p53-regulated miRNAs target transcription factors to regulate EMT

In 2007, the *miR-34* family was identified as the first miRNA directly regulated by p53 and shown to induce apoptosis and senescence (Chang et al., 2007; Corney et al., 2007; Raver-Shapira et al., 2007). Furthermore, ectopic p53 was shown to up-regulate miRNAs which regulate cell cycle, tumor metastasis and stemness by targeting transcription factors (Chang et al., 2011; Chen et al., 2013a; Sachdeva et al., 2009; Shimono et al., 2009; Xu et al., 2009).

EMT is a key process at early stages of metastasis (Thiery, 2002b). Besides the results described here, a number of other studies showed that p53 regulates EMT/MET through miRNA-mediated inhibition of transcription factors (Gregory et al., 2008; Hahn et al., 2013; Kim et al., 2011a; Kim et al., 2011b; Siemens et al., 2011). For example, p53-induced miR-34a represses EMT by decreasing SNAIL expression. Interestingly, ectopic SNAIL also down-regulates miR-34a in colorectal cancer cell lines (Siemens et al., 2011). These findings illustrate that miR-34a and SNAIL form a double-negative feedback loop, which is controlled by p53. In addition, Kim et al. showed that up-regulated miR-34 reduces Axin2 expression, which further increases GSK-3β nuclear location and leads to decreased SNAIL expression in colon cancer cells (Kim et al., 2013; Kim et al., 2011a). Furthermore, miR-34 can also regulate EMT through targeting another transcription factor, ZNF281, which is induced by SNAIL (Hahn et al., 2013). Moreover, ectopic miR-34a decreases the expression of the stem cell markers CD44 and Bmi1 (Siemens et al., 2011) indicating that stem cell-like features are also regulated by the p53/miR-34a axis.

It is known that c-MYC promotes EMT in cancer (Raver-Shapira et al., 2007; Sakuma et al., 2012; Smith et al., 2009), and studies reported that p53 could repress EMT through inducing the two tumor suppressor miRNAs miR-34 and miR-145 which both repress c-MYC (Christoffersen et al., 2010; Sachdeva et al., 2009).

Apart from the *miR-34* family, Kim *et al* found that the *miR-200* family, including miR-200a/b/c, miR-141 and miR-429, is induced by p53 (Kim et al., 2011b). The miR-200/ZEB1/2 axis is also involved in the negative regulation of EMT by p53 (Chang et al., 2011).

Previous results imply AP4 as a new mediator of EMT. Ectopic expression of AP4 directly represses E-Cadherin and induces SNAIL, VIM, N-cadherin and FOS in colon cancer cell lines (Jackstadt et al., 2013). AP4 is repressed by p53 in CRC cell lines, while miR-15a/16-1 levels are elevated. Here, we demonstrated that p53 decreases AP4 expression and inhibits EMT through inducing miR-15a/16-1. The details of the miR-15a/16-1/AP4 double-negative feedback loop are discussed below (see 5.2 and 5.3).

Previous studies showed that SNAIL is induced by AP4 and SNAIL represses miR-34a (Jackstadt et al., 2013; Siemens et al., 2011). Hence, miR-15a/16-1 may positively correlate with miR-34 by repressing AP4, which would presumably result in a decrease in SNAIL expression and de-repression of miR-34a. Indeed, Bandi *et al* reported that miR-15a/16-1 and miR-34 can co-operate in non-small cell lung cancer (Bandi and Vassella, 2011). Similarly, both miR-15a/16-1 and miR-200 regulate migration and invasion by targeting vascular endothelial growth factor (VEGF) (Roybal et al., 2011; Sun et al., 2013; Wang et al., 2012). Therefore, miR-15a/16-1 and miR-200 may co-regulate EMT through VEGF.

Taken together, our results indicate that the miR-15a/16-1/AP4 axis represents another p53/miRNAs/EMT-TF circuitry involved in the regulation of the EMT process. Moreover, miR-15a/16-1 may cooperate with miR-34 and

miR-200 to prevent erroneous loss of cellular differentiation due to aberrant signal, which may emanate from the cellular environment (Figure 25).

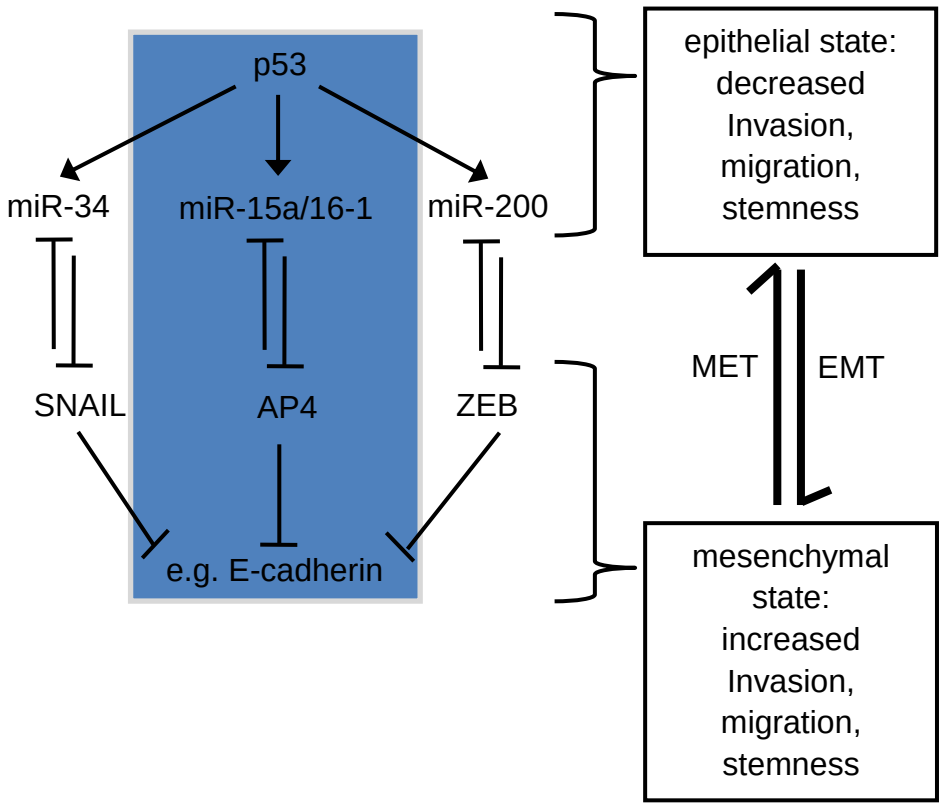

Figure 25 The regulation of EMT/MET by p53

The blue background indicates the miR-15a/16-1/AP4 circuitry involved in the regulation of EMT/MET and metastasis, which was identified in this thesis study. In addition, two more loops between EMT-TFs and p53-induced microRNAs are known, namely the miR-34a/SNAIL and miR-200/ZEB1/2 loops.

5.2 Repression of miR-15/16-1 by AP4

We employed an AP4 conditional expression system in the colon cancer cell line SW480 to show that AP4 can repress miR-15a/16-1 at both primary and mature miRNA levels. Next, we utilized ChIP and confirmed that there are two alternatives AP4 bound regions in the vicinity of *DLEU2* transcription start sites, the host gene of miR-15a/16-1. The results reveal that AP4 represses *DLEU2*

directly. Hence, miR-15a/16-1 and AP4 generate a double-negative feedback loop, similar to the previously reported miR-34/SNAIL1 and miR-200/ZEB1 feedback loops (Figure 25). The parallel presence of the three different loops may convey robustness to the system.

5.3 The role of the miR-15a/16-1/AP4 axis in EMT

As AP4 was described as a new EMT mediator in colon cancer (Jackstadt et al., 2013), we continued to focus on whether miR-15a/16-1 could regulate the EMT process by inhibiting AP4 expression. It is known that activated p53 represses EMT through the miR-34/SNAIL1 and miR-200/ZEB1/2 cascades. Here, we identified the miR-15a/16-1/AP4 double-negative feedback loop as an additional module regulated by p53. In addition, we also confirmed that ectopic expression of miR-15a/16-1 can induce MET in colorectal cancer cell lines. Similar results indicate that miR-16-1 may also regulate EMT in other types of cancer. Li *et al* reported that activated miR-16-1 represses migration and invasion in glioma cells (Li et al., 2013). Furthermore, ectopic miR-16-1 represses cell proliferation dramatically in U251 cells, but has no significant impact on cell apoptosis. However, the functional role of miR-15/16-1 in cell migration and invasion in this study is not fully understood.

Recently, Guo *et al* demonstrated that miR-15a inhibits EMT through the down-regulation of Bmi-1 (Guo et al., 2014). Bmi-1 expression decreases E-cadherin expression. However, the authors did not detect different expression of miR-16-1 in pancreatic cancer samples compared to normal pancreatic tissues.

Previous results showed miR-15a/16-1 is frequently deleted and regulates cell apoptosis and proliferation in cancer (Bandi et al., 2009; Calin et al., 2004; Chen et al., 2008; Lerner et al., 2009). However, how miR-15a/16-1 functions as a tumor suppressor is not fully understood. Here we show that miR-15a and

miR-16-1 reverses EMT in colon cancer and promotes MET. These findings suggest that down-regulation and/or inactivation of miR-15a/16-1 may contribute to tumor progression by promoting metastatic traits in addition to conteracting apoptosis and promoting cell proliferation.

5.4 The role of miR-15a/16-1/AP4 axis in cell cycle regulation

The mammalian cell division cycle, referred to as the cell cycle, is a strictly regulated process and a highly conserved pathway modulated by cyclin-dependent kinases (CDK). Several studies demonstrated that p21, which is induced by p53, connects p53 tightly to the cell cycle as it is a CDK inhibitor (Abbas and Dutta, 2009). Having established that activated AP4 represses p21 expression in the cell lines MCF-7 and U2OS (Jung et al., 2008), we assumed that miR-15a/16-1 could influence cell cycle progression by repressing AP4. Indeed, a G_1 arrest was observed after transfection of pre-miR-15a in SW480 cells. Concomitant expression of a conditional *AP4* allele lacking miR-15a seed-matching sequences attenuated the G_1 arrest mediated by miR-15a. This indicates that the cell cycle inhibitory function of miR-15a/16-1 requires repression of AP4.

miR-15a/16-1 was previously reported to induce a G_1 cell cycle arrest by repressing Cyclin D1 (CCND1). Interestingly, a truncation of *CCND1* mRNA which removes the seed-matching sites in the 3'-UTR, prevents repression by miR-15a in mantle cell lymphoma (Chen et al., 2008). Liu *et al.* implied that miR-15a/16-1 also represses cycle-dependent kinase (CDK) CDK6, CyclinD3 (CCND3) and Cyclin E1 (CCNE1) to inhibit G_1/S transition (Liu et al., 2008). Bandi *et al* showed that the regulation of cell cycle by miR-15a/16-1 in non-small cell lung cancer is dependent on the Retinoblastoma (Rb) protein (Bandi et al., 2009). E2F1 is a downstream target of Rb, and repressed by Rb. Ectopic E2F1 can induce G_1/S transition and unexpectedly promote

miR-15a/16-1 expression (Ofir et al., 2011). Therefore, miR-15a/16-1 may attenuate the influence of E2F1 in cell proliferation.

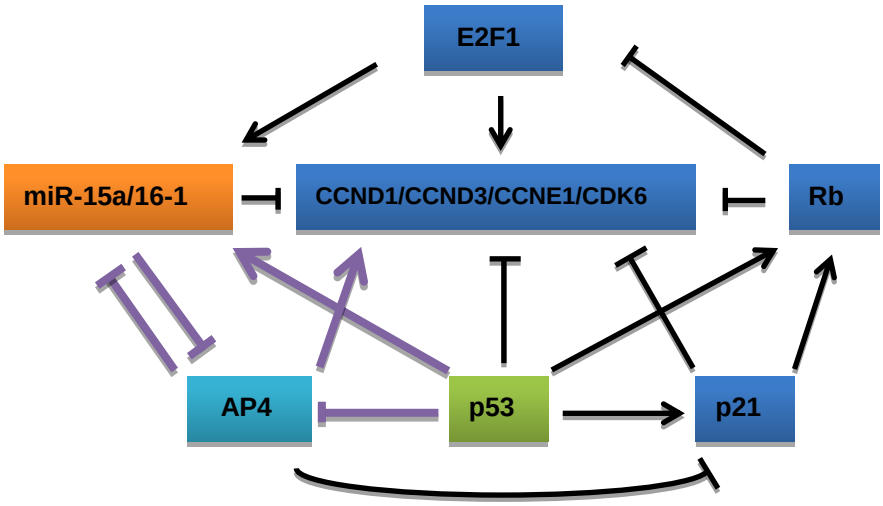

Figure26 The miR-15a/16-1/AP4 axis in the cell cycle regulation

miR-15a/16-1 regulates cell cycle through AP4 and other factors. Black arrows indicate previously described regulations, while purple arrows present the results from this study.

AP4 promotes cell cycle progression by repression of p21 (Jung et al., 2008). Furthermore, AP4 promotes cell cycle progression by repression of miR-15/16-1, which itself has a cell cycle inhibitory effect, in part by repressing AP4. Therefore, the tightly controlled balance between AP4 and miR-15a/16-1 levels may represent a critical component in the regulation of cell cycle progression, which is frequently disrupted during tumorigenesis (Figure 26).

5.5 The role of miR-15a/16-1/AP4 axis in experimental tumors

As described above, EMT is required for the initial step in metastasis formation and is necessary for extravasion. Therefore, we analyzed the impact of miR-15a/16-1 on the formation of lung metastasis by xenografted CRC cells in mice. Mice injected with SW620 cells expressing miR-15a/16-1 showed a

lower colonization in the lung and inhibits tumor formation *in vivo*.

Bonci *et al* reported that a knock-down of miR-15a/16-1 promotes prostate cell proliferation and tumorigenesis in immunodeficient NOD/SCID mice. Ectopic miR-15a/16-1 limits tumor growth in xenografts. WNT3A, which is correlated with tumor invasion, is repressed by miR-15a/16-1 (Bonci et al., 2008). Furthermore, monoclonal B cell lymphocytosis (MBL), CLL and Non-Hodgkin Lymphoma develop in miR-15a/16-1 knock-out mice. Of note, cell cycle mediators, like CCND2, CCND3, CDK4/6, are up-regulated in this system (Klein et al., 2010).

Collectively, these studies establish that miR-15a/16-1 has a tumor suppressor role *in vivo.* In addition, miR-15a and miR-16-1 regulate both cell cycle progression and EMT-related processes *in vivo*.

5.6 The correlation of miR-15a/16-1 and AP4 in clinical samples

Our results showed that miR-15a/16-1 and AP4 generate a double-negative feedback loop *in vitro*. Furthermore, we detected that miR-15a and AP4 display a negative correlation in human patient samples. In the dataset from Notterman *et al*, *AP4* expression negatively correlates with expression of the miR-15a/16-1 host gene *DLEU2* (Notterman et al., 2001). According to these results, *AP4* is increased in the samples of colorectal adenocarcinomas, while the *DLEU2* gene is down-regulated in the same stage of cancer. The reduced expression of miR-15a/16-1 in colon cancer may further cause the up-regulation of AP4, which can enhance EMT and promote metastasis.

Recently, Guo *et al* demonstrated that miR-15a expression negatively correlates with Bmi-1 expression in 42 pancreatic cancer samples (Guo et al., 2014). Furthermore, a decreased expression of Bmi-1 was associated with longer patient survival. In pancreatic cancer, higher expression of miR-15a was detected in pre-malignant tissues when compared to tumor tissues. Therefore,

the miR-15a/16-1 and AP4 loop may also be active in other types of cancer besides colorectal cancer.

Several studies showed that miR-15a/16-1 is frequently deleted and/or down-regulated in chronic lymphocytic leukemia. miR-15a/16-1 is located on chromosome 13q14.3. This 30-kb region is deleted or down-regulated in ~68% (41 in 60) of B cell chronic lymphocytic leukemia (B-CLL) (Calin et al., 2002). Liu *et al* demonstrated that the 13q14.3 deletion which contains the 10-kb MDR often occurs in CLL. The MDR harbors the promoter of miR-15a/16-1 host gene *DLEU2* (Figure4) (Liu et al., 1997).

5.7 miR-15a/16-1, AP4 and future perspective

Bmi-1 is one of the key regulators of stem cell maintenance and miR-15a/16-1 represses Bmi-1 expression in ovarian cancer (Bhattacharya et al., 2009). This implies that miR-15a/16-1 could also act as a regulator of stemness. Activated AP4 induces stem the cell markers CD44 and LGR5 in colon cancer cell lines. Therefore, miR-15a/16-1 may inhibit stemness by repressing AP4 and Bmi-1 in colon cancer cell lines.

miR-15a/16-1 is down-regulated in many kinds of cancers, like CLL, prostate, colon, and lung cancer (Bandi et al., 2009; Klein et al., 2010; Notterman et al., 2001). In contrast, AP4 promotes cell proliferation, induces EMT and metastasis *in vivo*. Therefore, a replacement therapy approach restoring expression of miR-15a/16-1 in humans could regulate multiple oncogenic signaling pathways. For example it could inhibit EMT through AP4, cell cycle progression via CCND1, stemness by targeting Bmi-1, and decrease VEGF signaling and affect angiogenesis. Collectively, these results suggest that restoring miR-15a/16-1 expression could be a promising therapeutic strategy. Interestingly, a trial with a similar replacement therapy approach is underway for miR-34 (Bader, 2012).

6 Summary

Previous results demonstrated that 13q14, the genomic location of *DLEU2,* which encodes the miR-15a/16-1 microRNAs, is deleted in more than 50% of chronic lymphatic leukemia (CLL) cases. miR-15a/16-1 down-regulates BCL2 and induces cell apoptosis. miR-15a/16-1 also inhibits cell cycle regulators, such as CCND1/3, CCNE2 and CDK2, thereby inducing a G_1 arrest. These data indicate that miR-15a and miR-16-1 may represent tumor suppressors. The Hermeking lab had recently described AP4 as a new inducer of EMT and tumor metastasis. Furthermore, AP4 was found to be repressed after DNA damage. In this thesis it was shown that this repression occurs in a p53-dependent manner. Since miR-15a/16-1 is induced by p53 and predicted to target the *AP4* 3'-UTR, we investigated whether and how miR-15a/16-1 could also exert its tumor suppressive function by repression of AP4. We determined that p53-induced miR-15a/16-1 directly represses AP4. Furthermore, miR-15/16-1 induces MET and promotes the epithelial state in the colorectal cancer cell line SW480. In addition, AP4 bound to the two alternative transcription start sites of *DLEU2* and represses miR-15a/16-1 expression. Therefore, miR-15a/16-1 and AP4 form a double-negative feedback loop similar to the previously reported miR-34/SNAIL and miR-200/ZEB1/2 loops, which are also regulated by p53.

In human colorectal cancer samples, miR-15a/16-1 showed a negative correlation with AP4 expression. In addition, xenograft experiments showed that stable expression of miR-15a/16-1 diminishes lung metastasis formation of colorectal cancer cells *in vivo*.

In conclusion, the findings of this study significantly enhance our understanding of the function of miR-15a/16-1 as a tumor suppressor in colon cancer. Additionally, the results indicate that replacement of miR-15a/16-1 could be a promising therapeutic strategy warranting further research.

7 Zusammenfassung

Vorherige Ergebnisse zeigten, dass die chromosomal Region 13q14, in der das *dLEU2* Gen liegt, welches die MikroRNAs miR-15a/16-1 kodiert, in mehr als 50% aller chronisch-lymphatischen Leukämien (CLL) deletiert vorliegt. miR-15a/16-1 induziert Apoptose indem es Bcl2 hemmt. Zudem hemmt miR-15a/16-1 die Zellzyklusregulatoren CCND1/3, CCNE2 und CDK2, wodurch es einen G1-Arrest induziert. Diese Daten zeigen, dass miR-15a und miR-16 Tumorsuppressoren darstellen. Das Hermeking Labor hat AP4 vor kurzem als neuen Induktor von EMT und Tumormetastasierung beschrieben. Zudem fanden sie, dass AP4 nach DNA-Schädigung herunterreguliert wird. In dieser Arbeit konnte gezeigt werden, dass dies in einer p53-abhängigen Weise geschieht. Da miR-15a/16-1 durch p53 induziert wird und der 3'-UTR von AP4 ein Ziel von miR-15a/16-1 ist, wurde untersucht, ob und wie miR-15a/16-1 seine Tumor-unterdrückende Funktion durch Repression durch AP4 vermittelt. Es konnte gezeigt werden, dass miR-15a/16-1 direkt AP4 unterdrückt. Außerdem, induziert ektopisches miR-15a/16-1 MET in der Darmkrebs-Zelllinie SW480. Desweiteren bindet AP4 an die zwei alternativen Transkriptionsstartstellen des *dLEU2* Gens und unterdrückt so die Expression von miR-15a/16-1. Somit bilden miR-15a/16-1 und AP4 eine negative Rückkopplungsschleife ähnlich den miR-34/SNAIL und miR-200/ZEB1/2 Schleifen, die auch durch p53 reguliert werden. In menschlichen Darmkrebspräparaten zeigte miR-15a/16-1 eine negative Korrelation mit AP4 Expression. Darüber hinaus resultierte die stabile Expression miR-15a/16-1 in kolorektalen Krebszellen in einer verminderten Bildung von Lungenmetastasen in xenotransplantierten Mäusen.

Die Ergebnisse dieser Studie tragen wesentlich zu unserem Verständnis der Funktion des Tumor-Suppressors miR-15a/16-1 bei Darmkrebs bei. Zusätzlich zeigen die Ergebnisse, dass die Rekonstitution von miR-15a/16-1 in Tumoren

ein vielversprechender therapeutischer Ansatz sein könnte, der weitere Forschung in dieser Richtung rechtfertigt.

8 Publications

The results of this thesis have been recently published:

Lei Shi*, Rene Jackstadt*, Helge Siemens, Huihui Li, Thomas Kirchner, Heiko Hermeking. p53-induced miR-15a/16-1 and AP4 form a double-negative feedback loop to regulate epithelial-mesenchymal transition and metastasis in colorectal cancer. Cancer Research. 2014 Jan 15; 74(2): 532-42.

(*: equally contributing first authors; Impact Factor 2013: 8.65)

9 References

Abbas, T., and Dutta, A. (2009). p21 in cancer: intricate networks and multiple activities. Nature reviews Cancer *9*, 400-414.

Akinyeke, T., Matsumura, S., Wang, X., Wu, Y., Schalfer, E. D., Saxena, A., Yan, W., Logan, S. K., and Li, X. (2013). Metformin targets c-MYC oncogene to prevent prostate cancer. Carcinogenesis *12*, 2823-32.

Al-Sohaily, S., Biankin, A., Leong, R., Kohonen-Corish, M., and Warusavitarne, J. (2012). Molecular pathways in colorectal cancer. Journal of gastroenterology and hepatology *27*, 1423-1431.

Aranburu, A., Carlsson, R., Persson, C., and Leanderson, T. (2001). Transcription factor AP-4 is a ligand for immunoglobulin-kappa promoter E-box elements. The Biochemical journal *354*, 431-438.

Arend, R. C., Londono-Joshi, A. I., Straughn, J. M., Jr., and Buchsbaum, D. J. (2013). The Wnt/beta-catenin pathway in ovarian cancer: A review. Gynecologic oncology *131*, 772-9.

Asangani, I. A., Rasheed, S. A., Nikolova, D. A., Leupold, J. H., Colburn, N. H., Post, S., and Allgayer, H. (2008). MicroRNA-21 (miR-21) post-transcriptionally downregulates tumor suppressor Pdcd4 and stimulates invasion, intravasation and metastasis in colorectal cancer. Oncogene *27*, 2128-2136.

Aulmann, S., Adler, N., Rom, J., Helmchen, B., Schirmacher, P., and Sinn, H. P. (2006). c-myc amplifications in primary breast carcinomas and their local recurrences. Journal of clinical pathology *59*, 424-428.

Bader, A. G. (2012). miR-34 - a microRNA replacement therapy is headed to the clinic. Frontiers in genetics *3*, 120.

Bae, Y., Kim, H., Namgoong, H., Baek, M., Lee, J., Hwang, D., Hwang, Y., Ahn, C., and Kang, S. (2001). Characterization of microsatellite markers adjacent to AP-4 on chromosome 16p13.3. Molecular and cellular probes *15*, 313-315.

Bandi, N., and Vassella, E. (2011). miR-34a and miR-15a/16 are co-regulated in non-small cell lung cancer and control cell cycle progression in a synergistic and Rb-dependent manner. Molecular cancer *10*, 55.

Bandi, N., Zbinden, S., Gugger, M., Arnold, M., Kocher, V., Hasan, L., Kappeler, A., Brunner, T., and Vassella, E. (2009). miR-15a and miR-16 are implicated in cell cycle regulation in a Rb-dependent manner and are frequently deleted or down-regulated in non-small cell lung cancer. Cancer research *69*, 5553-5559.

Bartel, D. P. (2004). MicroRNAs: genomics, biogenesis, mechanism, and function. Cell *116*, 281-297.

Bhattacharya, R., Nicoloso, M., Arvizo, R., Wang, E., Cortez, A., Rossi, S., Calin, G. A., and Mukherjee, P. (2009). MiR-15a and MiR-16 control Bmi-1 expression in ovarian cancer. Cancer research *69*, 9090-9095.

Bonci, D., Coppola, V., Musumeci, M., Addario, A., Giuffrida, R., Memeo, L., D'Urso, L., Pagliuca, A., Biffoni, M., Labbaye, C.*, et al.* (2008). The miR-15a-miR-16-1 cluster controls prostate cancer by targeting multiple oncogenic activities. Nature medicine *14*, 1271-1277.

Bourhis, J., Le, M. G., Barrois, M., Gerbaulet, A., Jeannel, D., Duvillard, P., Le Doussal, V., Chassagne, D., and Riou, G. (1990). Prognostic value of c-myc proto-oncogene overexpression in early invasive carcinoma of the cervix. Journal of clinical oncology : official journal of the American Society of Clinical Oncology *8*, 1789-1796.

Bowman, T., Broome, M. A., Sinibaldi, D., Wharton, W., Pledger, W. J., Sedivy, J. M., Irby, R., Yeatman, T., Courtneidge, S. A., and Jove, R. (2001). Stat3-mediated Myc expression is required for Src transformation and PDGF-induced mitogenesis. Proceedings of the National Academy of Sciences of the United States of America *98*, 7319-7324.

Bunz, F., Dutriaux, A., Lengauer, C., Waldman, T., Zhou, S., Brown, J. P., Sedivy, J. M., Kinzler, K. W., and Vogelstein, B. (1998). Requirement for p53 and p21 to sustain G2 arrest after DNA damage. Science *282*, 1497-1501.

Cader, F. Z., Vockerodt, M., Bose, S., Nagy, E., Brundler, M. A., Kearns, P., and Murray, P. G. (2013). The EBV oncogene LMP1 protects lymphoma cells from cell death through the collagen-mediated activation of DDR1. Blood *122*, 4237-45.

Calin, G. A., and Croce, C. M. (2006). Genomics of chronic lymphocytic leukemia microRNAs as new players with clinical significance. Seminars in oncology *33*, 167-173.

Calin, G. A., Dumitru, C. D., Shimizu, M., Bichi, R., Zupo, S., Noch, E., Aldler, H., Rattan, S., Keating, M., Rai, K.*, et al.* (2002). Frequent deletions and

down-regulation of micro- RNA genes miR15 and miR16 at 13q14 in chronic lymphocytic leukemia. Proceedings of the National Academy of Sciences of the United States of America *99*, 15524-15529.

Calin, G. A., Sevignani, C., Dumitru, C. D., Hyslop, T., Noch, E., Yendamuri, S., Shimizu, M., Rattan, S., Bullrich, F., Negrini, M., and Croce, C. M. (2004). Human microRNA genes are frequently located at fragile sites and genomic regions involved in cancers. Proceedings of the National Academy of Sciences of the United States of America *101*, 2999-3004.

Cappellen, D., Schlange, T., Bauer, M., Maurer, F., and Hynes, N. E. (2007). Novel c-MYC target genes mediate differential effects on cell proliferation and migration. EMBO reports *8*, 70-76.

Chang, C. J., Chao, C. H., Xia, W., Yang, J. Y., Xiong, Y., Li, C. W., Yu, W. H., Rehman, S. K., Hsu, J. L., Lee, H. H.*, et al.* (2011). p53 regulates epithelial-mesenchymal transition and stem cell properties through modulating miRNAs. Nat Cell Biol *13*, 317-323.

Chang, T. C., Wentzel, E. A., Kent, O. A., Ramachandran, K., Mullendore, M., Lee, K. H., Feldmann, G., Yamakuchi, M., Ferlito, M., Lowenstein, C. J.*, et al.* (2007). Transactivation of miR-34a by p53 broadly influences gene expression and promotes apoptosis. Molecular cell *26*, 745-752.

Chen, L., Zhang, R., Li, P., Liu, Y., Qin, K., Fa, Z. Q., Liu, Y. J., Ke, Y. Q., and Jiang, X. D. (2013a). P53-induced microRNA-107 inhibits proliferation of glioma cells and down-regulates the expression of CDK6 and Notch-2. Neuroscience letters *534*, 327-332.

Chen, R. W., Bemis, L. T., Amato, C. M., Myint, H., Tran, H., Birks, D. K., Eckhardt, S. G., and Robinson, W. A. (2008). Truncation in CCND1 mRNA alters miR-16-1 regulation in mantle cell lymphoma. Blood *112*, 822-829.

Chen, W. T., Zhu, G., Pfaffenbach, K., Kanel, G., Stiles, B., and Lee, A. S. (2013b). GRP78 as a regulator of liver steatosis and cancer progression mediated by loss of the tumor suppressor PTEN. Oncogene 2013 Oct 21, 1-9.

Chendrimada, T. P., Gregory, R. I., Kumaraswamy, E., Norman, J., Cooch, N., Nishikura, K., and Shiekhattar, R. (2005). TRBP recruits the Dicer complex to Ago2 for microRNA processing and gene silencing. Nature *436*, 740-744.

Cheng, A. M., Byrom, M. W., Shelton, J., and Ford, L. P. (2005a). Antisense inhibition of human miRNAs and indications for an involvement of miRNA in cell growth and apoptosis. Nucleic acids research *33*, 1290-1297.

Cheng, L. C., Tavazoie, M., and Doetsch, F. (2005b). Stem cells: from epigenetics to microRNAs. Neuron *46*, 363-367.

Chiorazzi, N., Rai, K. R., and Ferrarini, M. (2005). Chronic lymphocytic leukemia. The New England journal of medicine *352*, 804-815.

Christoffersen, N. R., Shalgi, R., Frankel, L. B., Leucci, E., Lees, M., Klausen, M., Pilpel, Y., Nielsen, F. C., Oren, M., and Lund, A. H. (2010). p53-independent upregulation of miR-34a during oncogene-induced senescence represses MYC. Cell death and differentiation *17*, 236-245.

Cimmino, A., Calin, G. A., Fabbri, M., Iorio, M. V., Ferracin, M., Shimizu, M., Wojcik, S. E., Aqeilan, R. I., Zupo, S., Dono, M.*, et al.* (2005). miR-15 and miR-16 induce apoptosis by targeting BCL2. Proceedings of the National Academy of Sciences of the United States of America *102*, 13944-13949.

Cui, Y., Narayanan, C. S., Zhou, J., and Kumar, A. (1998). Exon-I is involved in positive as well as negative regulation of human angiotensinogen gene expression. Gene *224*, 97-107.

De Craene, B., and Berx, G. (2013). Regulatory networks defining EMT during cancer initiation and progression. Nature reviews Cancer *13*, 97-110.

Duesberg, P. H., and Vogt, P. K. (1979). Avian acute leukemia viruses MC29 and MH2 share specific RNA sequences: evidence for a second class of transforming genes. Proceedings of the National Academy of Sciences of the United States of America *76*, 1633-1637.

Ebert, M. S., and Sharp, P. A. (2012). Roles for microRNAs in conferring robustness to biological processes. Cell *149*, 515-524.

Esquela-Kerscher, A., and Slack, F. J. (2006). Oncomirs - microRNAs with a role in cancer. Nature reviews Cancer *6*, 259-269.

Fabbri, M., Bottoni, A., Shimizu, M., Spizzo, R., Nicoloso, M. S., Rossi, S., Barbarotto, E., Cimmino, A., Adair, B., Wojcik, S. E.*, et al.* (2011). Association of a microRNA/TP53 feedback circuitry with pathogenesis and outcome of B-cell chronic lymphocytic leukemia. JAMA : the journal of the American Medical Association *305*, 59-67.

Fearon, E. R., and Vogelstein, B. (1990). A genetic model for colorectal tumorigenesis. Cell *61*, 759-767.

Feliciano, A., Castellvi, J., Artero-Castro, A., Leal, J. A., Romagosa, C., Hernandez-Losa, J., Peg, V., Fabra, A., Vidal, F., Kondoh, H.*, et al.* (2013). miR-125b acts as a tumor suppressor in breast tumorigenesis via its novel direct targets ENPEP, CK2-alpha, CCNJ, and MEGF9. PloS one *8*, e76247.

Fleming, N. I., Jorissen, R. N., Mouradov, D., Christie, M., Sakthianandeswaren, A., Palmieri, M., Day, F., Li, S., Tsui, C., Lipton, L.*, et al.* (2013). SMAD2, SMAD3 and SMAD4 mutations in colorectal cancer. Cancer research *73*, 725-735.

Fodde, R., and Brabletz, T. (2007). Wnt/beta-catenin signaling in cancer stemness and malignant behavior. Current opinion in cell biology *19*, 150-158.
Friedman, R. C., Farh, K. K., Burge, C. B., and Bartel, D. P. (2009). Most mammalian mRNAs are conserved targets of microRNAs. Genome research *19*, 92-105.

Gabriely, G., Wurdinger, T., Kesari, S., Esau, C. C., Burchard, J., Linsley, P. S., and Krichevsky, A. M. (2008). MicroRNA 21 promotes glioma invasion by targeting matrix metalloproteinase regulators. Molecular and cellular biology *28*, 5369-5380.

Gong, J., Zhang, J. P., Li, B., Zeng, C., You, K., Chen, M. X., Yuan, Y., and Zhuang, S. M. (2013). MicroRNA-125b promotes apoptosis by regulating the expression of Mcl-1, Bcl-w and IL-6R. Oncogene *32*, 3071-3079.

Gregory, P. A., Bert, A. G., Paterson, E. L., Barry, S. C., Tsykin, A., Farshid, G., Vadas, M. A., Khew-Goodall, Y., and Goodall, G. J. (2008). The miR-200 family and miR-205 regulate epithelial to mesenchymal transition by targeting ZEB1 and SIP1. Nature cell biology *10*, 593-601.

Guo, S., Xu, X., Tang, Y., Zhang, C., Li, J., Ouyang, Y., Ju, J., Bie, P., and Wang, H. (2014). miR-15a inhibits cell proliferation and epithelial to mesenchymal transition in pancreatic ductal adenocarcinoma by down-regulating Bmi-1 expression. Cancer letters *344*, 40-46.

Hadjihannas, M. V., Bruckner, M., Jerchow, B., Birchmeier, W., Dietmaier, W., and Behrens, J. (2006). Aberrant Wnt/beta-catenin signaling can induce chromosomal instability in colon cancer. Proceedings of the National Academy of Sciences of the United States of America *103*, 10747-10752.

Hahn, S., Jackstadt, R., Siemens, H., Hunten, S., and Hermeking, H. (2013). SNAIL and miR-34a feed-forward regulation of ZNF281/ZBP99 promotes epithelial-mesenchymal transition. The EMBO journal *32*, 3079-95.

Han, J., Lee, Y., Yeom, K. H., Nam, J. W., Heo, I., Rhee, J. K., Sohn, S. Y., Cho, Y., Zhang, B. T., and Kim, V. N. (2006). Molecular basis for the recognition of primary microRNAs by the Drosha-DGCR8 complex. Cell *125*, 887-901.

Hermeking, H. (2012). MicroRNAs in the p53 network: micromanagement of tumour suppression. Nat Rev Cancer *12*, 613-626.

Hollstein, M., Sidransky, D., Vogelstein, B., and Harris, C. C. (1991). p53 mutations in human cancers. Science *253*, 49-53.

Hu, S. S., Lai, M. M., and Vogt, P. K. (1979). Genome of avian myelocytomatosis virus MC29: analysis by heteroduplex mapping. Proceedings of the National Academy of Sciences of the United States of America *76*, 1265-1268.

Hu, Y. F., Luscher, B., Admon, A., Mermod, N., and Tjian, R. (1990). Transcription factor AP-4 contains multiple dimerization domains that regulate dimer specificity. Genes & development *4*, 1741-1752.

Imai, K., and Okamoto, T. (2006). Transcriptional repression of human immunodeficiency virus type 1 by AP-4. The Journal of biological chemistry *281*, 12495-12505.

Jackstadt, R., Roh, S., Neumann, J., Jung, P., Hoffmann, R., Horst, D., Berens, C., Bornkamm, G. W., Kirchner, T., Menssen, A., and Hermeking, H. (2013). AP4 is a mediator of epithelial-mesenchymal transition and metastasis in colorectal cancer. The Journal of experimental medicine *210*, 1331-1350.

Jaganathan, S., Yue, P., Paladino, D. C., Bogdanovic, J., Huo, Q., and Turkson, J. (2011). A functional nuclear epidermal growth factor receptor, SRC and Stat3 heteromeric complex in pancreatic cancer cells. PloS one *6*, e19605.

Jung, P., and Hermeking, H. (2009). The c-MYC-AP4-p21 cascade. Cell Cycle *8*, 982-989.

Jung, P., Menssen, A., Mayr, D., and Hermeking, H. (2008). AP4 encodes a c-MYC-inducible repressor of p21. Proceedings of the National Academy of Sciences of the United States of America *105*, 15046-15051.

Kim, N. H., Cha, Y. H., Kang, S. E., Lee, Y., Lee, I., Cha, S. Y., Ryu, J. K., Na, J. M., Park, C., Yoon, H. G*., et al.* (2013). p53 regulates nuclear GSK-3 levels through miR-34-mediated Axin2 suppression in colorectal cancer cells. Cell Cycle *12*, 1578-1587.

Kim, N. H., Kim, H. S., Li, X. Y., Lee, I., Choi, H. S., Kang, S. E., Cha, S. Y., Ryu, J. K., Yoon, D., Fearon, E. R.*, et al.* (2011a). A p53/miRNA-34 axis regulates Snail1-dependent cancer cell epithelial-mesenchymal transition. The Journal of cell biology *195*, 417-433.

Kim, T., Veronese, A., Pichiorri, F., Lee, T. J., Jeon, Y. J., Volinia, S., Pineau, P., Marchio, A., Palatini, J., Suh, S. S.*, et al.* (2011b). p53 regulates epithelial-mesenchymal transition through microRNAs targeting ZEB1 and ZEB2. The Journal of experimental medicine *208*, 875-883.

Klein, U., Lia, M., Crespo, M., Siegel, R., Shen, Q., Mo, T., Ambesi-Impiombato, A., Califano, A., Migliazza, A., Bhagat, G., and Dalla-Favera, R. (2010). The DLEU2/miR-15a/16-1 cluster controls B cell proliferation and its deletion leads to chronic lymphocytic leukemia. Cancer cell *17*, 28-40.

Larsson, L. G., and Henriksson, M. A. (2010). The Yin and Yang functions of the Myc oncoprotein in cancer development and as targets for therapy. Experimental cell research *316*, 1429-1437.

Laurent-Puig, P., Agostini, J., and Maley, K. (2010). [Colorectal oncogenesis]. Bulletin du cancer *97*, 1311-1321.

Lee, J., Ballikaya, S., Schonig, K., Ball, C. R., Glimm, H., Kopitz, J., and Gebert, J. (2013). Transforming growth factor beta receptor 2 (TGFBR2) changes sialylation in the microsatellite unstable (MSI) Colorectal cancer cell line HCT116. PloS one *8*, e57074.

Lee, R. C., Feinbaum, R. L., and Ambros, V. (1993). The C. elegans heterochronic gene lin-4 encodes small RNAs with antisense complementarity to lin-14. Cell *75*, 843-854.

Lerner, M., Harada, M., Loven, J., Castro, J., Davis, Z., Oscier, D., Henriksson, M., Sangfelt, O., Grander, D., and Corcoran, M. M. (2009). DLEU2, frequently deleted in malignancy, functions as a critical host gene of the cell cycle inhibitory microRNAs miR-15a and miR-16-1. Experimental cell research *315*, 2941-2952.

Levine, A. J., Finlay, C. A., and Hinds, P. W. (2004). P53 is a tumor suppressor gene. Cell *116*, S67-S70.

Li, X., Ling, N., Bai, Y., Dong, W., Hui, G. Z., Liu, D., Zhao, J., and Hu, J. (2013). MiR-16-1 plays a role in reducing migration and invasion of glioma cells. Anatomical record *296*, 427-432.

Liu, H., Radisky, D. C., Yang, D., Xu, R., Radisky, E. S., Bissell, M. J., and Bishop, J. M. (2012). MYC suppresses cancer metastasis by direct transcriptional silencing of alphav and beta3 integrin subunits. Nat Cell Biol *14*, 567-574.

Liu, Q., Fu, H., Sun, F., Zhang, H., Tie, Y., Zhu, J., Xing, R., Sun, Z., and Zheng, X. (2008). miR-16 family induces cell cycle arrest by regulating multiple cell cycle genes. Nucleic acids research *36*, 5391-5404.

Liu, Y., Corcoran, M., Rasool, O., Ivanova, G., Ibbotson, R., Grander, D., Iyengar, A., Baranova, A., Kashuba, V., Merup, M.*, et al.* (1997). Cloning of two candidate tumor suppressor genes within a 10 kb region on chromosome 13q14, frequently deleted in chronic lymphocytic leukemia. Oncogene *15*, 2463-2473.

Lujambio, A., and Lowe, S. W. (2012). The microcosmos of cancer. Nature *482*, 347-355.

Lund, E., Guttinger, S., Calado, A., Dahlberg, J. E., and Kutay, U. (2004). Nuclear export of microRNA precursors. Science *303*, 95-98.

Luscher, B., and Larsson, L. G. (1999). The basic region/helix-loop-helix/leucine zipper domain of Myc proto-oncoproteins: function and regulation. Oncogene *18*, 2955-2966.

Mani, S. A., Guo, W., Liao, M. J., Eaton, E. N., Ayyanan, A., Zhou, A. Y., Brooks, M., Reinhard, F., Zhang, C. C., Shipitsin, M.*, et al.* (2008). The epithelial-mesenchymal transition generates cells with properties of stem cells. Cell *133*, 704-715.

Mermod, N., Williams, T. J., and Tjian, R. (1988). Enhancer binding factors AP-4 and AP-1 act in concert to activate SV40 late transcription in vitro. Nature *332*, 557-561.

Meyer, N., and Penn, L. Z. (2008). Reflecting on 25 years with MYC. Nature reviews Cancer *8*, 976-990.

Notterman, D. A., Alon, U., Sierk, A. J., and Levine, A. J. (2001). Transcriptional gene expression profiles of colorectal adenoma, adenocarcinoma, and normal tissue examined by oligonucleotide arrays. Cancer research *61*, 3124-3130.

Ofir, M., Hacohen, D., and Ginsberg, D. (2011). MiR-15 and miR-16 are direct transcriptional targets of E2F1 that limit E2F-induced proliferation by targeting cyclin E. Molecular cancer research *9*, 440-447.

Park, J. Y., Singh, T. R., Nassar, N., Zhang, F., Freund, M., Hanenberg, H., Meetei, A. R., and Andreassen, P. R. (2013). Breast cancer-associated missense mutants of the PALB2 WD40 domain, which directly binds RAD51C, RAD51 and BRCA2, disrupt DNA repair. Oncogene 2013 Oct 21, 1-10.

Roybal, J. D., Zang, Y., Ahn, Y. H., Yang, Y., Gibbons, D. L., Baird, B. N., Alvarez, C., Thilaganathan, N., Liu, D. D., Saintigny, P.*, et al.* (2011). miR-200 Inhibits lung adenocarcinoma cell invasion and metastasis by targeting Flt1/VEGFR1. Molecular cancer research *9*, 25-35.

Ruegger, S., and Grosshans, H. (2012). MicroRNA turnover: when, how, and why. Trends in biochemical sciences *37*, 436-446.

Rustgi, A. K. (2013). BRAF: a driver of the serrated pathway in colon cancer. Cancer cell *24*, 1-2.

Sachdeva, M., Zhu, S., Wu, F., Wu, H., Walia, V., Kumar, S., Elble, R., Watabe, K., and Mo, Y. Y. (2009). p53 represses c-Myc through induction of the tumor suppressor miR-145. Proceedings of the National Academy of Sciences of the United States of America *106*, 3207-3212.

Sakuma, K., Aoki, M., and Kannagi, R. (2012). Transcription factors c-Myc and CDX2 mediate E-selectin ligand expression in colon cancer cells undergoing EGF/bFGF-induced epithelial-mesenchymal transition. Proceedings of the National Academy of Sciences of the United States of America *109*, 7776-7781.

Savagner, P., Boyer, B., Valles, A. M., Jouanneau, J., and Thiery, J. P. (1994). Modulations of the epithelial phenotype during embryogenesis and cancer progression. Cancer Treat Research 71, 229-249.

Shi, L., Jackstadt, R., Siemens, H., Li, H., Kirchner, T., and Hermeking, H. (2014). p53-Induced miR-15a/16-1 and AP4 Form a Double-Negative Feedback Loop to Regulate Epithelial-Mesenchymal Transition and Metastasis in Colorectal Cancer. Cancer research *74*, 532-542.

Shimono, Y., Zabala, M., Cho, R. W., Lobo, N., Dalerba, P., Qian, D., Diehn, M., Liu, H., Panula, S. P., Chiao, E.*, et al.* (2009). Downregulation of miRNA-200c links breast cancer stem cells with normal stem cells. Cell *138*, 592-603.

Siemens, H., Jackstadt, R., Hunten, S., Kaller, M., Menssen, A., Gotz, U., and Hermeking, H. (2011). miR-34 and SNAIL form a double-negative feedback loop to regulate epithelial-mesenchymal transitions. Cell Cycle *10*, 4256-4271.

Siemens, H., Neumann, J., Jackstadt, R., Mansmann, U., Horst, D., Kirchner, T., and Hermeking, H. (2013). Detection of miR-34a promoter methylation in combination with elevated expression of c-Met and beta-catenin predicts distant metastasis of colon cancer. Clin Cancer Res *19*, 710-720.

Smith, A. P., Verrecchia, A., Faga, G., Doni, M., Perna, D., Martinato, F., Guccione, E., and Amati, B. (2009). A positive role for Myc in TGFbeta-induced Snail transcription and epithelial-to-mesenchymal transition. Oncogene *28*, 422-430.

Sun, C. Y., She, X. M., Qin, Y., Chu, Z. B., Chen, L., Ai, L. S., Zhang, L., and Hu, Y. (2013). miR-15a and miR-16 affect the angiogenesis of multiple myeloma by targeting VEGF. Carcinogenesis *34*, 426-435.

Sur, S., Pagliarini, R., Bunz, F., Rago, C., Diaz, L. A., Jr., Kinzler, K. W., Vogelstein, B., and Papadopoulos, N. (2009). A panel of isogenic human cancer cells suggests a therapeutic approach for cancers with inactivated p53. Proceedings of the National Academy of Sciences of the United States of America *106*, 3964-3969.

Suzuki, H. I., Yamagata, K., Sugimoto, K., Iwamoto, T., Kato, S., and Miyazono, K. (2009). Modulation of microRNA processing by p53. Nature *460*, 529-533.

Thiery, J. P. (2002a). Epithelial-mesenchymal transitions in tumour progression. Nature reviews Cancer *2*, 442-454.

Thiery, J. P. (2002b). Epithelial–mesenchymal transitions in tumour progression. Nature Reviews Cancer *2*, 442-454.

Thiery, J. P., Acloque, H., Huang, R. Y., and Nieto, M. A. (2009). Epithelial-mesenchymal transitions in development and disease. Cell *139*, 871-890.

Tsai, J. H., Donaher, J. L., Murphy, D. A., Chau, S., and Yang, J. (2012). Spatiotemporal regulation of epithelial-mesenchymal transition is essential for squamous cell carcinoma metastasis. Cancer cell *22*, 725-736.

Tsujimoto, K., Ono, T., Sato, M., Nishida, T., Oguma, T., and Tadakuma, T. (2005). Regulation of the expression of caspase-9 by the transcription factor activator protein-4 in glucocorticoid-induced apoptosis. The Journal of biological chemistry *280*, 27638-27644.

Vousden, K. H., and Prives, C. (2009). Blinded by the Light: The Growing Complexity of p53. Cell *137*, 413-431.

Wang, Y., Fan, H., Zhao, G., Liu, D., Du, L., Wang, Z., Hu, Y., and Hou, Y. (2012). miR-16 inhibits the proliferation and angiogenesis-regulating potential of mesenchymal stem cells in severe pre-eclampsia. The FEBS journal *279*, 4510-4524.

Wightman, B., Ha, I., and Ruvkun, G. (1993). Posttranscriptional regulation of the heterochronic gene lin-14 by lin-4 mediates temporal pattern formation in C. elegans. Cell *75*, 855-862.

Xu, N., Papagiannakopoulos, T., Pan, G., Thomson, J. A., and Kosik, K. S. (2009). MicroRNA-145 regulates OCT4, SOX2, and KLF4 and represses pluripotency in human embryonic stem cells. Cell *137*, 647-658.

Xu, Y. Z., Kanagaratham, C., Jancik, S., and Radzioch, D. (2013). Promoter deletion analysis using a dual-luciferase reporter system. Methods in molecular biology *977*, 79-93.

Zhu, S., Wu, H., Wu, F., Nie, D., Sheng, S., and Mo, Y. Y. (2008). MicroRNA-21 targets tumor suppressor genes in invasion and metastasis. Cell research *18*, 350-359.

Acknowledgment

First of all, I give my sincerest gratitude to my supervisor Prof. Dr. rer. nat. Heiko Hermeking. Thank you for the invaluable scientific suggestions and discussions. Thank you for everything you provided to me. At beginning of my time in Germany, I met a lot of trouble and could not adjust myself into the non-mother country quickly. Even I had to change to a new lab. It was you who accepted me in your lab and gave me enough time to continue the project. You provided me a challenging and exciting research topic, countless insightful comments and guidance. You have consistently been a constant source of inspiration and support throughout my Ph.D study. I have learned from you what the characteristics of a real scientist are. Your passion for science and perseverance on achievement will encourage me forever.

My sincere thanks to all colleagues and co-workers at the Institute of Pathology for their kind help in research and life. Special thanks goes to the following colleagues:

Thanks a lot, Dr. Rene Jackstadt. You are more than a colleague. You are an advisor as well as a friend. Without your advice, I could not manage everything successfully.

Sincere thanks also goes to Dr. Helge Siemens for his support and many interesting conversations.

Dr. Markus Kaller I would also like to thank for all his advice and patients.

Stefanie Hahn and Sabine Hünten, thanks a lot for all your help and explaining organizational things.

Ursula Goetz, thanks for kindly technical support.

Dr. Matjaz Rokavec thanks for being such a great colleague.

Hereby, my special thanks to goes Longchang Jiang and Huihui Li. Jiang, it is you, with whom I had lunch together each day. It is you, who sent me a lot of funny messages and pictures which I can smile often. Thank you a lot. I will certainly remember every detail of the past 3 years we shared together.

Curriculum Vitae

Name: Shi Lei
Date of Birth: 1982.12.16 (Hebei, China PRC)

Education:

2011.1- Now Dr. rer. nat. candidate student, Molecular and Experimental Pathology, Institute of Pathology,
Ludwig-Maximilians-Universität München, Munich, Germany
Supervisor: Prof. Dr. rer. nat. Heiko Hermeking

2007.9- 2010.6 Master degree of Vet Microbiology
College of Veterinary Medicine,
Huazhong Agricultural University, Wuhan, Hubei, China.
Supervisor: Prof. Aizhen Guo D.V.M & Ph.D.

2003.9- 2007.6 Bachelor of Veterinary Medicine
College of Animal Science, Heibei North University, Zhang Jiakou, Hebei, China.

Research Experience:

2011.1- now Pathology Institute, LMU Munich,
p53-induced miR-15a/16-1 and AP4 form a double-negative feedback loop to regulate epithelial-mesenchymal transition and metastasis in colorectal cancer

2008.5- 2010.06 National Key Laboratory of Agricultural Microbiology, HZAU
Preliminary research on the identification of the pathogen, diagnosis and vaccine on *Mycoplasma. Bovis* Penumonia

2008.2- 2008.5 Beijing Tuberculosis and Thoracic Tumor Research Institute
Different transcriptional profiling between dendritic cells infected with virulent and avirulent mycobacteria in BSL-3 laboratory.

2007.3- 2007.5 College of Veterinary Medicine, HZAU
Bachelor thesis: Development and primary application of indirect ELISA for detection antibodies against Mycobacterium bovis

Poster presentations / Meeting attendance:

1. AACR 105thAnnual Meeting 2014, 2014.04.05-09. San Diego, California, US.
Poster presentation: p53-induced miR-15a/16-1 and AP4 form a double-negative feedback loop to regulate epithelial-mesenchymal transition and metastasis in colorectal cancer

2. 97. Jahrestagung der Deutschen Gesellschaft for Pathology, 2013.05.23-26. Heidelberg. Germany (attended)

Publications:

1. Lei Shi*, Rene Jackstadt*, Helge Siemens, Huihui Li, Thomas Kirchner, Heiko Hermeking. p53-induced miR-15a/16-1 and AP4 form a double-negative feedback loop to regulate epithelial-mesenchymal transition and metastasis in colorectal cancer. Cancer Research. 2014 Jan 15; 74(2): 532-42.

2. **Lei Shi**, Gong Rui, Yin Zheng-yan, Zhou Yong, Pei Jie, Hu Zhi-bin, Wang Li-xia, Hu Changmin, Liu Tao, Chen Yingyu, Liao Juanhong, Zhao Junlong, Chen Huan-chun, Guo Ai-zhen. Prelinminary Diagnosis of Cattle Infectious Mycoplasma bovis Pneumonia. Chinese Journal of Diagnosis of Agricultural University (Natural Science Edition), Aug. 2008. 27(4), 572.

3. **Lei Shi,** Gong Rui, Yin Zheng-yan, Zhou Yong, Pei Jie, Hu Zhi-bin, Wang Li-xia, Hu Changmin, Liu Tao, Chen Yingyu, Liao Juanhong, ZHAO Junlong, Chen Huanchun, GUO Aizhen. Diagnosis of Cattle Infectious Mycoplasma bovis Pneumonia. Chinese Journal of Huazhong Agricultural University (Natural Science Edition), Oct. 2008, 27(5), 629～633.

4. Hu Changmin, **Lei Shi**, Gong Rui, Bai Zhidi, Guo Aizhen. Progress on Mycoplasma bovis. Chinese Journal of Progress in Veterinary Medicine. 2009, 30(8): 73-77.

5. Hu Changmin, Liu Tao, **Lei Shi**, Zhang Minmin, Peng Qingjie, Guo Aizhen. The nutrition and hazard of distiller's grains as the forage. Chinese paper publishedon the proceedings of the 24th Congress of Chinese Breeding Society & The first National Congress of Cow Diseases.

6. Rui Gong, Changmin Hu, Haiyang Xu, Aizhen Guo, Huanchun Chen, Guangzhi Zhang, and **Lei Shi**. Evaluation of Clumping Factor A Binding Region A in a Subunit Vaccine against *Staphylococcus aureus*-Induced Mastitis in Mice. Clinical and Vaccine Immunology, November 2010, Vol. 17, No. 11 p. 1746-1752.

7. Jingjing Qi, Aizhen Guo, Peng Cui, Yingyu Chen, Mustafa Riaz, Xiaoliang Ba, Changmin Hu, Zhidi Bai, Xi Chen, **Lei Shi**, Huanchun Chen. Comparative geno-plasticity analysis of Mycoplasma bovis HB0801 (Chinese isolate). PLoS One, May 2012, Vol 7, Issue 5, e38239.